European Journal of Pharmaceutical Sciences 187 (2023) 106461

Contents lists available at ScienceDirect

European Journal of Pharmaceutical Sciences

journal homepage: www.elsevier.com/locate/ejps

Utilization of a kinetic isotope effect to decrease decomposition of ceftriaxone in a mixture of D_2O/H_2O

Ivona Jasprica [a,*], Petar Horvat [a], Katarina Zrnc [a], Karl J. Bonney [b], Vidar Bjornstad [b], Lucija Hok [c], Robert Vianello [c], Nikola Bregović [d], Josip Požar [d], Katarina Leko [d], Vladislav Tomišić [d], Ernest Meštrović [a,*]

[a] Xellia Ltd., Slavonska avenija 24/6, Zagreb 10000, Croatia
[b] Xellia Pharmaceuticals AS, Silurveien 2, Oslo 0380, Norway
[c] Laboratory for the Computational Design and Synthesis of Functional Materials, Ruđer Bošković Institute, Bijenička 54, Zagreb, Croatia
[d] Department of Chemistry, Faculty of Science, Horvatovac 102A, Zagreb, Croatia

ARTICLE INFO

Keywords:
β-lactams
Ceftriaxone
D_2O kinetic isotope effect
Molecular dynamics simulations
Quantum-chemical calculations

ABSTRACT

The discovery of cephalosporin and demonstration of its improved stability in aqueous solution, as well as enhanced *in vitro* activity against penicillin-resistant organisms, were major breakthroughs in the development of β-lactam antibiotics. Although cephalosporins are more stable with respect to hydrolytic degradation than penicillins, they still experience a variety of chemical transformations. The present study offers an insight into the rates and mechanisms of ceftriaxone degradation at the therapeutic concentration in water, a mixture of water and deuterium oxide, and deuterium oxide itself at the neutral pH.

Specific ceftriaxone degradation products were observed in aged samples (including a previously unreported dimer-type species), and by comparing the degradation rates in H_2O and D_2O, the observation of a kinetic isotope effect provided some valuable insight as to the nature of the initial ceftriaxone degradation. The effect of protium to deuterium isotope change on the degradation kinetics of ceftriaxone was evaluated using the method of initial rates based on HPLC analysis as well as by quantitative ^{1}H NMR spectroscopy. Moreover, computational analysis was utilized to get a molecular insight into chemical processes governing the ceftriaxone degradation and to rationalize the stabilizing effect of replacing H_2O with D_2O.

1. Introduction

Since their discovery in the 1920s, β-lactam antibiotics have played a prominent role in the fight against bacterial diseases. Although β-lactams are essential antibiotics, their instability in solution was, and still is, a significant obstacle to their development as active pharmaceutical ingredients and as different finished dosage forms.

The labile β-lactam ring of penicillins and other β-lactam antibiotics is characterized by its pronounced susceptibility to various nucleophiles, acid-base reagents, oxidizing agents or even solvents like water and alcohol. The stability or rate of degradation of different β-lactam members *in vivo* as well as *in vitro* is quite different. However, the major pathways of their degradation are similar, leading to various breakdown products (Deshpande et al., 2004).

The discovery of cephalosporin from the culture of *C. acremonium* in 1945 by Brotzu (Bo, 2000), and demonstration of its improved stability in aqueous solution (even at pH = 2), as well as its enhanced *in vitro* activity against penicillin-resistant organisms by Abraham and Newton (Hamilton-Miller, 2000), were major breakthroughs in the history of β-lactam antibiotics. Although cephalosporins are shown to be more stable to hydrolytic degradation reactions than penicillins, they still experience a variety of chemical and enzymatic transformations (Frau et al., 1997; Yamana and Tsuji, 1976).

The present study was designed to gain insight into the kinetics of cephalosporin degradation, more specifically, ceftriaxone degradation at its therapeutic concentration. Ceftriaxone is one of the essential

Abbreviations: CEF, ceftriaxone; CEFNa, ceftriaxone sodium; HPLC, high-performance liquid chromatography; MS, mass spectrometry; MS/MS, tandem mass spectrometry; WFI, water for injection; KIE, kinetic isotope effect; SKIE, solvent kinetic isotope effect; NMR, nuclear magnetic resonance; DFT, density-functional theory; RC, reactive complex.

* Corresponding authors.
E-mail addresses: Ivona.Jasprica@xellia.com (I. Jasprica), Ernest.Mestrovic@xellia.com (E. Meštrović).

https://doi.org/10.1016/j.ejps.2023.106461
Received 3 April 2023; Accepted 7 May 2023
Available online 7 May 2023

parenterally administered cephalosporins and is a broad-spectrum β-lactam antibiotic used for the treatment of bacterial infections of the respiratory tract, skin, soft tissue, and urinary tract. It has a very long half-life compared to other cephalosporins and is highly penetrable into the meninges, eyes, and inner ear. Ceftriaxone has broader and stronger gram-negative coverage than first or second-generation cephalosporins, but weaker activity against methicillin-susceptible *S. aureus*. Organisms that are generally susceptible to ceftriaxone include *S. pneumoniae, S. pyogenes* (group A β-hemolytic streptococci), coagulase-negative staphylococci, some Enterobacter spp, *H. influenzae, N. gonorrhoeae, P. mirabilis, E. coli, Klebsiella* spp, *M. catarrhalis, B. burgdorferi*, and some oral anaerobes (Richards et al., 1984).

Ceftriaxone works by inhibiting the mucopeptide synthesis in the bacterial cell wall, and its structure is presented in Fig. 1.

The β-lactam moiety of ceftriaxone binds to carboxypeptidases, endopeptidases, and transpeptidases in the bacterial cytoplasmic membrane. These enzymes are involved in cell-wall synthesis and cell division. Binding of ceftriaxone to these enzymes causes the enzyme to lose activity; therefore, the bacteria produce defective cell walls, causing cell death. Ceftriaxone is administered as a sodium salt at the therapeutic concentration of 20 mg mL^{-1}, 40 mg mL^{-1} or 100 mg mL^{-1}, and is only given as an injection, either intramuscularly or intravenously. Ceftriaxone is less than 1% bioavailable if given orally (Richards et al., 1984).

A literature search was performed to gain insight into the degradation pathways of different cephalosporins. The comparative stability of six cephalosporins (but not ceftriaxone) in aqueous solution (kinetics and mechanism of degradation) was studied in 1976 by Yamana and Tsuji, (Yamana and Tsuji, 1976) and degradation pathways specific for each molecule were proposed.

Ceftriaxone degradation in aqueous solution was studied and described by Zajac and Muszalska (Zając and Muszalska, 1998). Kinetic interpretation and proposals for the neutral, acid- and base-catalyzed hydrolysis pathways of ceftriaxone in aqueous media are presented in the aforementioned paper. Studies were done in the concentration range of 0.4 mg of ceftriaxone disodium per mL up to 0.8 mg mL^{-1} (significantly lower than the therapeutic concentrations). More precisely, degradation of ceftriaxone was studied at two different temperatures at pH 0.42, 7.38 and 13.22. According to the authors, in the early stage of hydrolysis the principal degradation product isolated in acidic, basic, and neutral solutions was identified as 5,6-dioxo-4-hydro-2-hydroxy-3--methyl-1,3,4-triazine (otherwise called degradation product B; structure presented in Fig. 2).

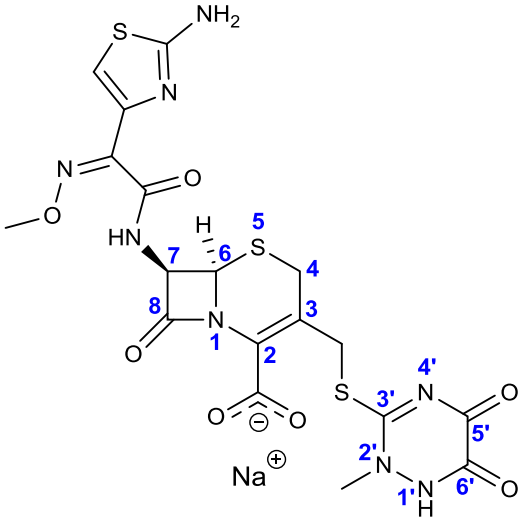

Fig. 1. Structure of ceftriaxone sodium (with numbering of the bicyclic core and triazine).

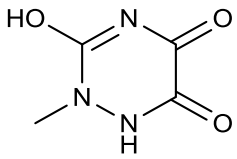

Fig. 2. Degradation product B.

Furthermore, according to the authors, in the first stage of ceftriaxone hydrolysis, the CH_2-S bond is cleaved (presumably by S_N2 attack of water) to form -CH_2OH at C-3 under acidic to basic conditions. In the basic solution the formation and reversible lactonization of products A and C was then noted (named as such by Zajac and Muszalska; the structures of these impurities are presented in Figs. 3 and 4). Structures A and C differ in the stereochemistry at C-7, where A has undergone epimerization at this position. In this second stage of the ceftriaxone degradation, opening of the β-lactam ring and simultaneous epimerization at C-7 and lactonization of the C-4 carboxyl and C-3 CH_2OH group were observed in basic solution. The opened β-lactam ring degradation product was not observed in the acidic conditions (product D, Fig. 5).

Product E, probably an isomer of the *N*-oxime function in Ceftriaxone, was observed in the acidic and neutral conditions (structure presented in Fig. 6).

Ceftriaxone isomerization in aqueous solution was also studied by Tian et al., using a ceftriaxone reference standard at the concentration of 3.0 mg mL^{-1} (Tian et al., 2015). The authors observed reversible isomerization and discussed its mechanism. The results reported in this article confirm that in an acidic aqueous solution, Ceftriaxone undergoes hydrolysis of the group at C-3 (with the thiol equivalent of the compound in Fig. 2 being observed), and it also undergoes a previously unknown reversible epimerization. The authors proposed that the isomerization mechanism involves nucleophilic attack of N-5′ on C-3, which is more pronounced in the presence of weaker acids. The proposed isomerization mechanism is presented in Fig. 7.

In addition to the abovementioned studies, Abramović et al. (2021) have experimentally and computationally investigated the process of hydrolysis and photolysis of cephalosporin antibiotics, with ceftriaxone as a model compound. According to the authors, an aqueous solution of ceftriaxone is reportedly unstable; its stability is pH and temperature dependent, and degradation occurs according to multiple pathways. Although unstable, because ceftriaxone is a clinical commonly used antibiotic, it is accumulated in the water, and therefore causes a lot of ecological, environmental, and health issues. Therefore, the authors investigated ceftriaxone hydrolysis in ultrapure and natural water to evaluate its behavior in the environment. A study was performed on a relatively low ceftriaxone concentration (0.05 mM, i.e., 0.000027 mg mL^{-1}) to mimic its presence in the environment. It was found that ceftriaxone hydrolysis in natural water was five and three times slower than in ultrapure water, at 25 °C and 4 °C respectively.

In addition to Abramović et al. (2021), degradation of ceftriaxone in the environment (soil samples) was studied by Jiang et al. (2010). The authors found that hydrolysis of ceftriaxone in water is significantly faster when exposed to light, indicating that direct photolysis is the primary process of ceftriaxone elimination from the surface water.

All of the aforementioned papers gave insightful information into possible ceftriaxone degradation pathways, but at concentrations that are significantly lower than therapeutically administered. As ceftriaxone is one of the most frequently used parenteral antibiotics in treating specific infections, understanding of its degradation mechanisms at the concentration administered parenterally is essential for development of formulations containing this API. Therefore, our study was focused on further increasing the knowledge of ceftriaxone behavior in the aqueous environment at the therapeutic concentration of 20 mg mL^{-1} which can be parenterally administered to patients. The study was directed towards obtaining kinetic information on the rates and mechanisms of

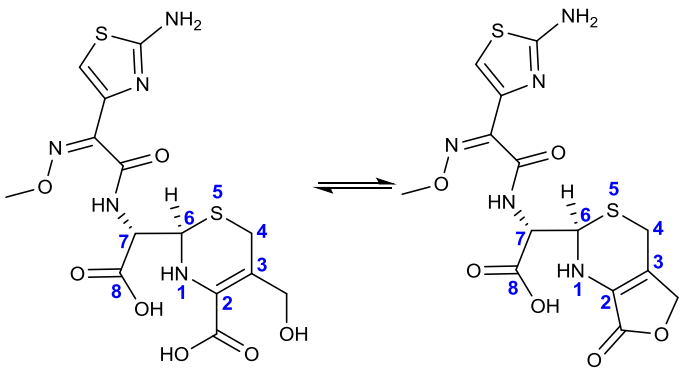

Fig. 3. Structure of degradation product A (left) and its lactonized form (right), as proposed by Zając and Muszalska (1998).

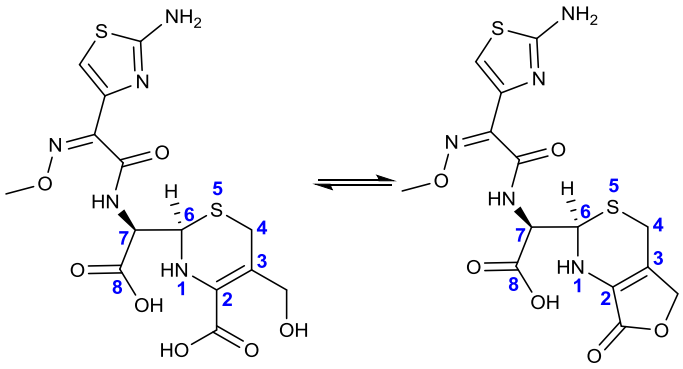

Fig. 4. Structure of degradation product C (left) and its lactonized form (right), as proposed by Zając and Muszalska (1998).

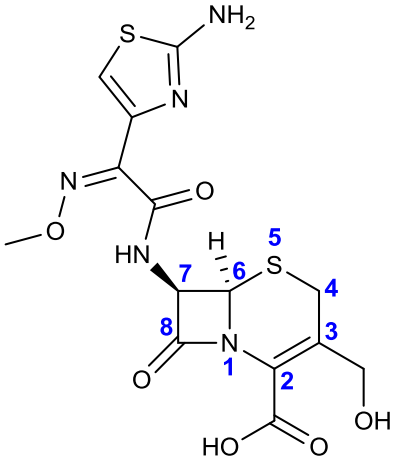

Fig. 5. Structure of degradation product D, as proposed by Zając and Muszalska (1998).

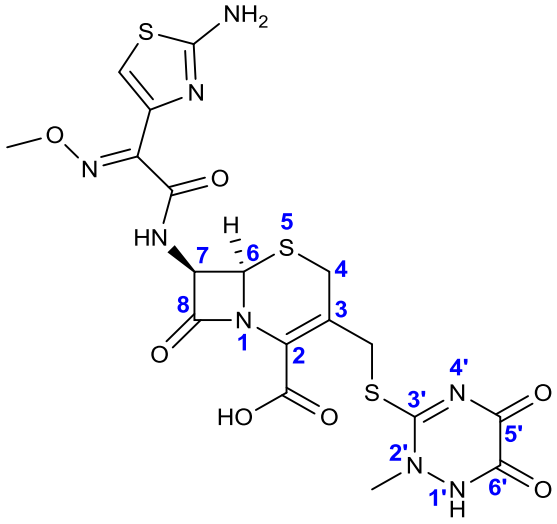

Fig. 6. Structure of degradation product E (designated as such by Zając and Muszalska (1998).

ceftriaxone degradation in water, a mixture of water and deuterium oxide, and deuterium oxide itself at neutral pH (range of 6.7 to 7.6). Previously, Yamana et al. (1977) studied the deuterium solvent isotope effect on penicillin G degradation rate. Still, to the best of our knowledge, such a study has not been published for cephalosporins, or more specifically, for ceftriaxone.

Specific ceftriaxone degradation products were observed in aged samples prepared in water, deuterium oxide, and a mixture of water and deuterium oxide using HPLC and MS methodology. By comparing the degradation rates in H_2O and D_2O, the observation of a kinetic isotope effect (KIE) provided some valuable insight to the nature of the initial degradation of ceftriaxone. This result, in combination with an investigation of the reaction order for the degradation using the method of initial rates, highlighted the important contribution of the formation of a previously unreported dimer-type species (from here on the term 'Dimer' refers to a compound with a mass of 949, corresponding to $2M^{-}159$, where M is the mass of ceftriaxone).

Specific degradation pathways, e.g., lactam ring-opening, lactone formation, nucleophilic displacement of 2-methyl-3-sulfanyl-1,2-dihydro-1,2,4-triazin-5,6-dione (referred in the text before as ceftriaxone Impurity C) with water, and the formation of Dimer are proposed. Some specific pathways agree with already published data (as discussed

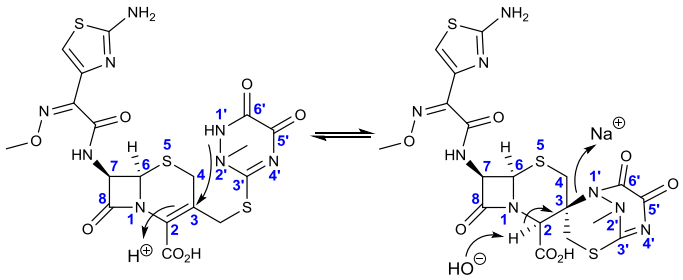

Fig. 7. Mechanism of isomerization proposed by Tian et al. (2015).

below), but for example, the hypothesized dimerization was, to the best of our knowledge, not published before. Hypothesized mechanisms are presented as a part of the Results and discussion section (proposed structures are shown in Fig. 8 below).

2. Result and discusion

2.1. Stability of ceftriaxone in water and deuterium oxide (HPLC analysis)

The stability of ceftriaxone samples prepared as described above, in Water for Injection (WFI), a predefined mixture of WFI and deuterium oxide (D_2O), or just D_2O, was evaluated during a predefined period at a predefined temperature. Ceftriaxone stability in specific formulations was assessed both through the decrease of the ceftriaxone assay measured at a particular timepoint compared to the ceftriaxone assay measured at the time of preparation, and through monitoring the formation of specific degradation products. Samples were analyzed using HPLC, where structures of specific impurities were determined using HPLC and compared to appropriate standards, or were proposed based on MS and MS/MS. The pH of the samples was also recorded at the start, and every tested stability point.

According to the data presented in Table 1, it can be concluded that as the proportion of D_2O in the formulation increases, the degradation of ceftriaxone in the samples exposed to the same stability testing conditions decreases (the assay decrease is lower, as well as the content of impurities). The impurity profile of different samples (prepared in WFI, a predefined mixture of WFI and D_2O, or D_2O) tested using the same conditions seems to be similar, with the amount of specific impurities (Impurity 242, Triazine impurity, and Dimer) decreasing as the proportion of D_2O increases.

Fig. 8 presents the proposed ceftriaxone degradation pathway in an aqueous environment at a therapeutic concentration of 20 mg mL^{-1}.

The structure of the impurity with the exact mass of 159 Da (designated in Fig. 8 as Triazine impurity) is a known impurity of ceftriaxone listed in the pharmacopoeias (known as ceftriaxone Impurity C). Impurity 242 corresponds to cefepime Impurity C, but to our knowledge, Dimer was never described before and represents a new degradation impurity of ceftriaxone.

The structure of the newly identified ceftriaxone impurity, Dimer, was proposed (as presented in Fig. 9). MS/MS fragmentation supports the proposed structure, with main fragments corresponding to structures in Fig. 9. A fragment with *m/z* 791 corresponds to loss of the triazine ring, while the fragment with *m/z* 747 is a result of further loss of CO_2 from the thiazine ring. Cleavege of the C-C and C-N bonds in the β lactam ring leads to fragment *m/z* 636. Cleavege of the C-N bond between thiazole ring and dihydrothiazine ring leads to fragment *m/z* 396, and further loss of water and carbon monoxide results in fragment *m/z* 352. From *m/z* 352 further fragmentation to *m/z* 396, *m/z* 241, *m/z* 156, *m/z* 126 and *m/z* 112 is identical to fragmentation of Ceftriaxone (Fig. 10).

2.2. Kinetic study results

In order to gain more insight into the early stages of the degradation pathway(s), we decided to investigate the role of water in more depth by exploring the kinetics when the hydrogen in water is replaced by the heavier deuterium.

Experiments were set up in H_2O and D_2O and samples were stored at 25 °C, with the ceftriaxone concentration being assessed daily by HPLC assay. There was no pH adjustment carried out either before or during the study, which in H_2O means that the initial pH was 6.7. The method of initial rates was used for this study, meaning that only the first 10% of ceftriaxone degradation is considered, and first-order reaction kinetics was assumed in the rate constant calculations.

The results show that there is clearly a difference in the rate of degradation in H_2O compared to D_2O, giving a KIE of 1.84 ± 0.09 (Fig. 11). This is a relatively large effect, with the magnitude indicating a primary kinetic isotope effect, meaning that an O-H bond in water is broken in the rate determining step in the initial degradation of ceftriaxone. This indicates that there is a key protonation prior to further

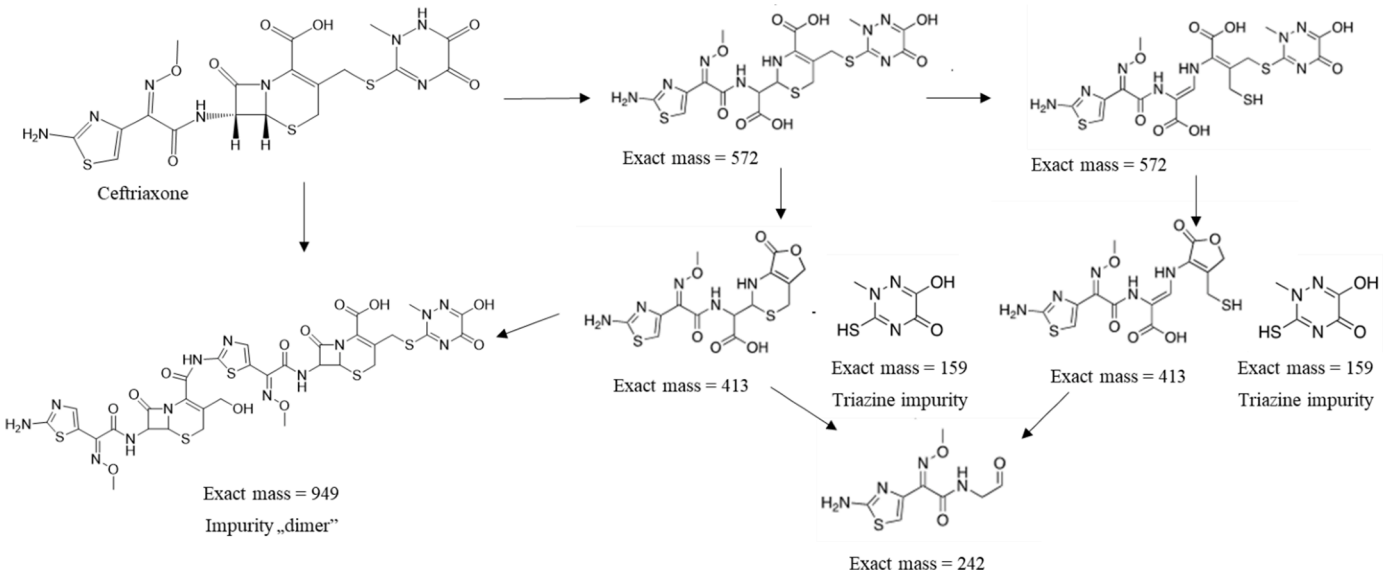

Fig. 8. Proposed ceftriaxone degradation pathway in an aqueous environment at 20 mg mL-1 concentration. Structures of impurities detected in analyzed samples, together with respective molecular masses, are proposed.

Table 1
Results of stability testing of ceftriaxone samples (20 mg mL^{-1} prepared in WFI, a predefined mixture of WFI and D_2O, or D_2O) loaded on stability for a predefined period at a predefined temperature.

Sample	Testing Point (days)	Temperature (°C)	pH**	Impurities content (%)			ΔAssay drop (%)***
				Imp. 242	Triazine Imp.*	Dimer Imp.	
CEFNa in WFI	START	/	6.74	<0.10	/	<0.10	/
	1	40	6.88	1.03	2.47	0.99	10.4
	2	40	6.85	1.86	4.65	1.11	19.4
	7	25	7.81	1.14	2.60	0.80	9.8
	14	15	7.31	0.65	1.59	0.65	7.7
	30	2–8	6.99	0.24	0.64	0.40	3.4
	60	2–8	6.97	0.56	1.27	0.55	6.7
CEFNa in a mixture of 50% WFI (V/V) and 50% D_2O (V/V)	0	/	7.07	<0.10	/	<0.10	/
	1	40	7.16	0.69	2.00	1.03	8.7
	2	40	7.10	1.31	3.75	1.36	16.7
	7	25	7.80	0.80	1.99	0.88	7.6
	14	15	7.35	0.48	1.22	0.70	6.3
	30	2–8	7.01	0.19	0.46	0.38	2.5
	60	2–8	7.00	0.38	0.91	0.54	5.5
CEFNa in D_2O	0	/	7.05	<0.10	/	<0.10	/
	1	40	7.24	0.40	1.55	1.10	6.7
	2	40	7.23	0.73	2.85	1.46	12.9
	7	25	7.79	0.47	1.49	0.94	5.3
	14	15	7.40	0.28	0.90	0.72	4.7
	30	2–8	7.05	0.11	0.32	0.36	1.6
	60	2–8	6.97	0.23	0.63	0.52	3.8

* Triazine impurity chemical name is 3-Mercapto-2-methyl-1,2-dihydro-1,2,4-triazine-5,6-dione;.
** pH is reported as measured by a pH meter, no corrections for pD were made;.
*** Ceftriaxone assay drop is calculated as the absolute value of the difference between the ceftriaxone assay at the specific stability testing point and the assay at the start.

reactivity, or that there is a key protonation, with concurrent attack by a nucleophile for example, in the rate determining step.

At the concentration used, the pH of ceftriaxone is found to increase over time as degradation occurs, stabilizing at approximately pH 7.5. Therefore, an additional study was carried out in which the initial pH in H_2O was increased to 7.5 by the addition of sodium hydroxide, and the equivalent was achieved in D_2O by the addition of sodium deuteroxide. The same initial concentration, temperature, and sampling rate was used as the first study (Fig. 12).

Although the rate of initial degradation in H_2O was very similar, taking 5.82 ± 0.69 days to reach 10% degradation when starting at pH 6.7 and 5.31 ± 0.35 days when starting at pH 7.5, the KIE was lower in this study at 1.41 ± 0.14. This is in line with the hypothesis that a key protonation is involved in promoting degradation at around neutral pH, and the potential for this process decreases as the pH increases.

We then switched focus to explore the role of ceftriaxone itself in the degradation (Fig. 13). A study was carried out to investigate the observed reaction order for the degradation of ceftriaxone. The method of initial rates was again used, with focus on the first 10% of degradation. Experiments were carried out with 20, 30, 40, 60 and 80 mg mL^{-1} concentrations of ceftriaxone in H_2O, with the temperature maintained at 25 °C and no pH adjustment either before or during the study. The ceftriaxone concentration in each experiment was again assessed daily by HPLC assay. When the ln rate of ceftriaxone degradation is plotted against the ln of the initial ceftriaxone concentration, it reveals an observed reaction order of 1.21 ± 0.04.

Interestingly, formation of the Dimer is lower when starting at pH 6.7 than when starting at pH 7.5. This observation, along with the KIE being smaller at the higher pH, indicates that formation of this compound involves a protonation event in the rate determining step. The mass of the Dimer is 949, which is equivalent to 2M-159, where M is the mass of ceftriaxone, and 159 is the mass of Triazine Impurity. Therefore, it seems likely that one ceftriaxone molecule attacks the carbon atom of the CH_2-S attached as C-3, displacing Triazine Impurity. This bimolecular reaction would explain the contribution of second order kinetics observed in the experimentally determined reaction order, and a plausible structure for the Dimer is presented in Fig. 14.

2.3. NMR study

In order to assess the effect of protium to deuterium isotope change on the degradation kinetics of ceftriaxone at several solvent compositions, i.e. several D_2O/H_2O ratios, we performed a series of kinetic experiments using quantitative ^1H NMR as the method for monitoring the time dependence of CEF concentration. Solvents containing D_2O and H_2O in various percentages (10, 25, 50, 75 and 100%, $V(D_2O)/V(H_2O)$) were examined. The initial values of pH and ceftriaxone concentration were for all experiments 6.8 and 0.036 M, respectively. The experiments were carried out at 25 and 40 °C with the total duration of typically 20 days at 40 °C and 30 days at 25 °C. The assay decreases measured by this methodology were in a good agreement with those obtained by HPLC with the same conditions and reaction times.

During the monitored reaction period, the change in ceftriaxone concentration was more than 50%. The collected data was processed by assuming first-order degradation kinetics. Such an approach yielded a good agreement of the experimental and calculated data (Figs. 15 and 16), providing the corresponding rate constants (Table 2). This suggested that the effect of the second-order degradation process (detected by initial-rate method, see above) is relatively small at such a low initial CEF concentration and the degradation proceeds primarily via the pathway which obeys the first-order rate law.

The degradation rate constant was in clear correlation with the solvent composition, i.e. the amount of D_2O present in the system. The dependence of k on the percentage of D_2O could be satisfactorily described by a linear function (Fig. 17). The slope of the straightline was rather similar for both temperatures. Such an empirical function could be rather useful to estimate the rate constant at any solvent composition containing D_2O and H_2O in variable fractions. Within this work, this fact was utilized to determine the rate constant in pure H_2O. Namely, the rate constant could not be directly measured for pure H_2O as a solvent by means of NMR due to the requirements of deuterium presence to allow for lock of the magnetic field. However, this value could be estimated as the intercept of the straight-line with the ordinate and the corresponding values are presented in Table 2. Based on the gathered data, the solvent kinetic isotope effect (SKIE) could be calculated and it amounted to 1.7

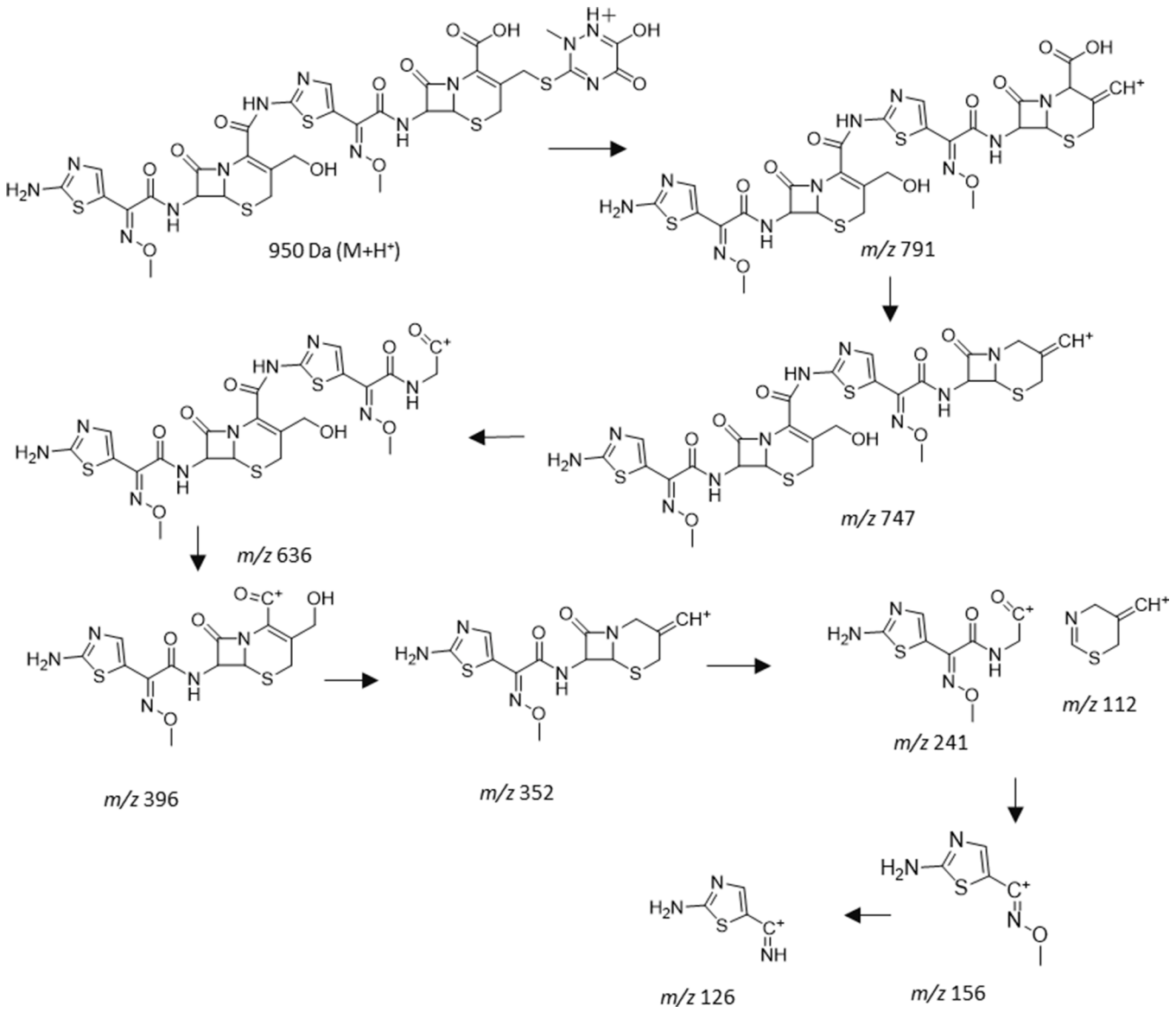

Fig. 9. Fragmentation of ceftriaxone Dimer impurity.

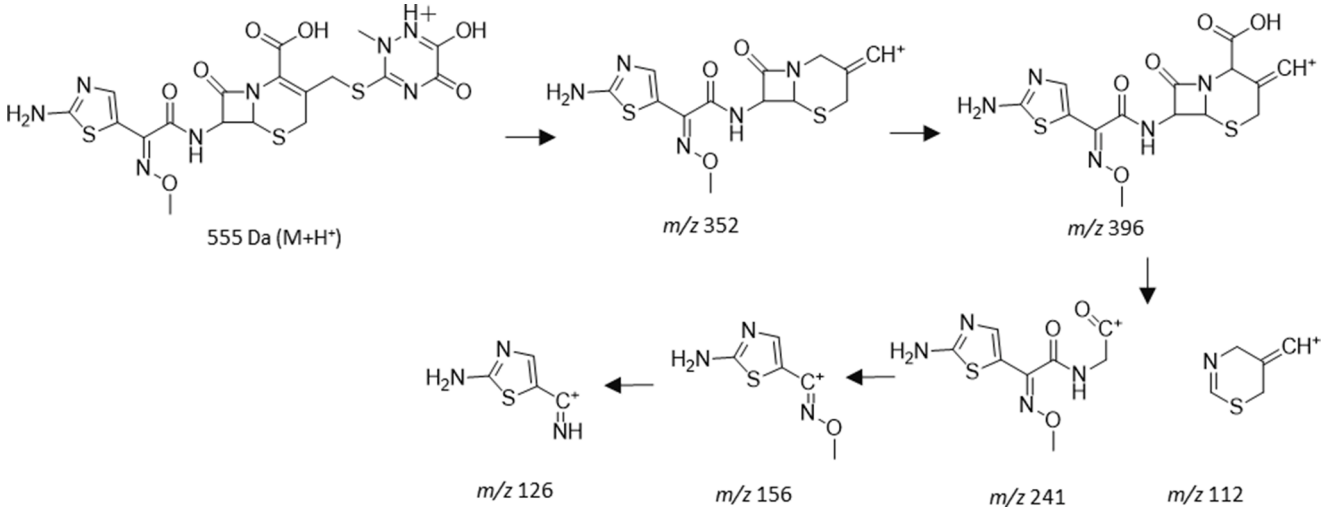

Fig. 10. MS/MS fragmentation of Ceftriaxone.

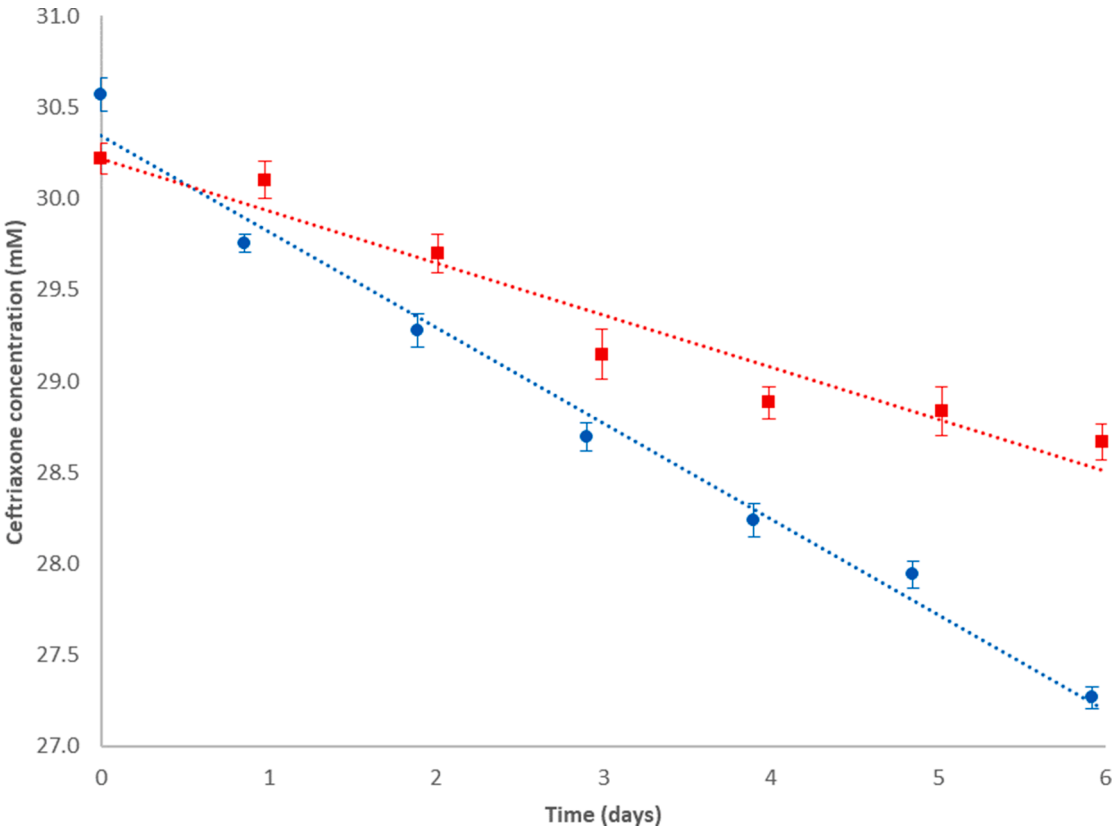

Fig. 11. Degradation rate of ceftriaxone in H_2O and D_2O starting at pH 6.7 (experiments, sampling and HPLC analysis were all carried out in triplicate; error bars are at the 99.5% confidence level; R^2 values are 0.985 (H_2O) and 0.941 (D_2O); ● H_2O, ■ D_2O).

(1) at 25 °C and 2.6(1) at 40 °C. This result was in good agreement with the one determined by HPLC at 25 °C, in which case the value of 1.88 was found. That is again in line with the assumption that a primary kinetic isotope effect governs the solvent effect on the degradation of CEF in the studied systems.

2.4. Computational analysis results

Computational analysis was utilized to get a molecular insight into chemical processes governing the ceftriaxone (CEF) degradation and to rationalize the effect of replacing H_2O with D_2O on its increased stability. For that purpose, we carried out molecular dynamics simulations in both explicit solvents and a range of mechanistic DFT calculations to obtain the underlying kinetic and thermodynamic parameters of the most prevailing reactions in solution. In doing so, we focused on two dominant processes, namely (i) the opening of the β-lactam ring following the hydrolytic cleavage of its C–N amide bond, and (ii) the breaking of the C–S bond linking the triazine moiety with the rest of the structure (Fig. 18). While the first process represents a degradation route common to β-lactam antibiotics (Waterman et al., 2002) and various other amides (East, 2018), the second route is more specific to CEF and is afforded by the good leaving group ability of its triazine. The starting point of our calculations was the dianionic form of CEF, given its determined pK_a values of 2.37 and 4.21 for the deprotonation of carboxylic and triazine units (Aleksić et al., 2005), respectively, which suggest a predominance of their deprotonated states under employed conditions. Other than those, the same literature advises that the aminothiazole basicity and the free amide acidity are linked with the pK_a values of 3.03 and 10.74, thus indicating that conditions exceeding those studied here are required for these processes to occur, which is why they were not considered in any detail.

2.5. β–Lactam ring opening

Hydrolytic opening of the β-lactam amide is a typical degradation route for this kind of compounds, which cleaves the corresponding N–C bond, thereby affording a carboxylate and an amine (Table 3). This instability is attributed to the strain in the lactam ring and its non-planarity, which inhibits the usual amide resonance. Accordingly, the rates of the β-lactam hydrolysis significantly exceed those for larger and less strained cyclic lactams, while these are all typically more vulnerable than their acyclic analogues (Wan et al., 1980). This makes it reasonable to expect a significant contribution of this process to the overall degradation products.

Under neutral conditions (Table 3, pH = 7), the formation of a reactive complex (RC) with water requires 3.4 kcal mol^{-1} and another 24.1 kcal mol^{-1} to arrive at the transition state (TS1) for the formation of the tetrahedral intermediate (IN1). The latter still preserves the amide N–C bond at 1.54 Å, yet being 0.18 Å longer than in the isolated CEF, where it is 1.36 Å. This process is assisted with the neighboring carboxylate through a simultaneous proton abstraction from the incoming water, which increases its nucleophilicity and promotes the reaction. With this in mind, we note that such a design of the CEF structure that allows a catalytic carboxylate in the immediate vicinity of the reaction center, is likely responsible for a larger susceptibility of CEF (and other similar β–lactam antibiotics) towards this degradation process at pH = 7 relative to simpler amides, where such a moiety is absent. As an illustration, at pH = 7, the hydrolysis of formamide is linked with $\Delta G^{\ddagger} = 34.7$ kcal mol^{-1} (East, 2018) and is significantly more difficult to occur.

The formed intermediate IN1 is unstable and quickly ruptures the amide bond into carboxylic and anionic amine moieties (IN2), over a barrier of only 2.7 kcal mol^{-1}. The latter is also positioned high on the free energy scale and is subsequently stabilized by two spontaneous

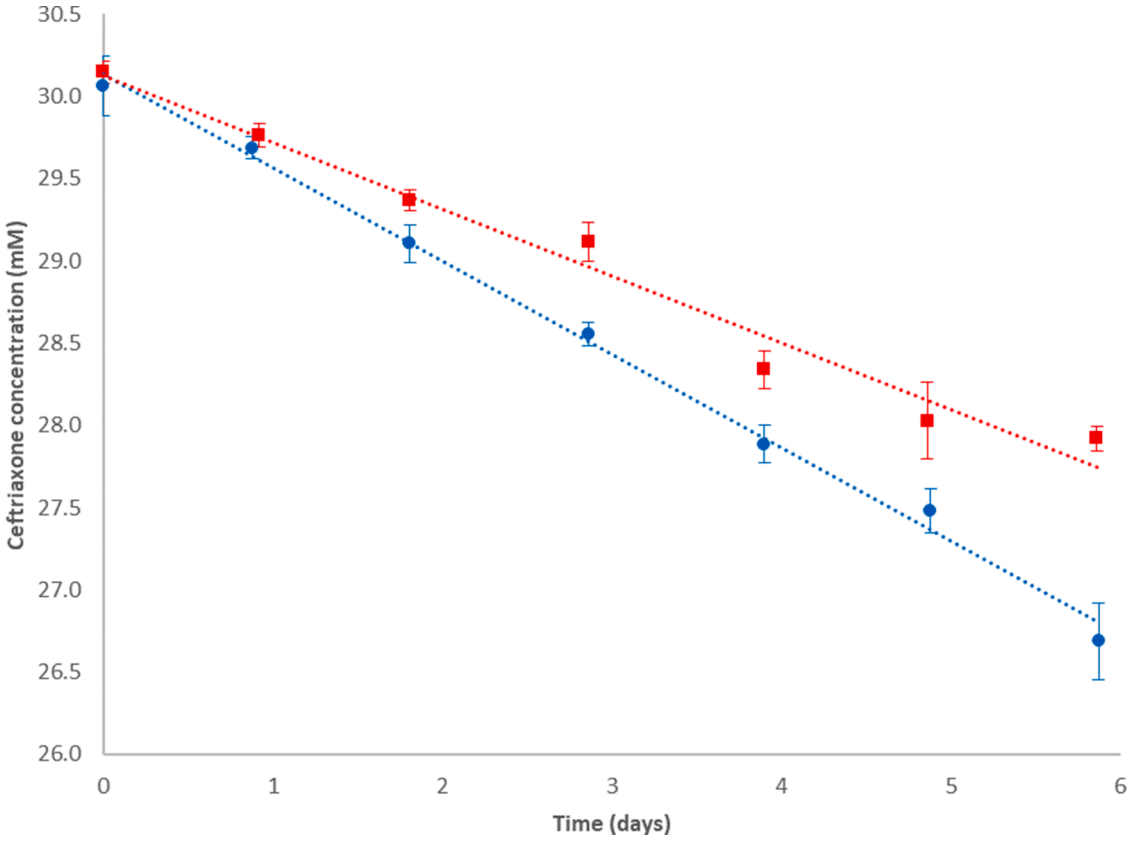

Fig. 12. Degradation rate of ceftriaxone in H_2O and D_2O starting at pH 7.5 (experiments, sampling and HPLC analysis were all carried out in triplicate; error bars are at the 99.5% confidence level; R^2 values are 0.996 (H_2O) and 0.976 (D_2O); ● H_2O, ■ D_2O).

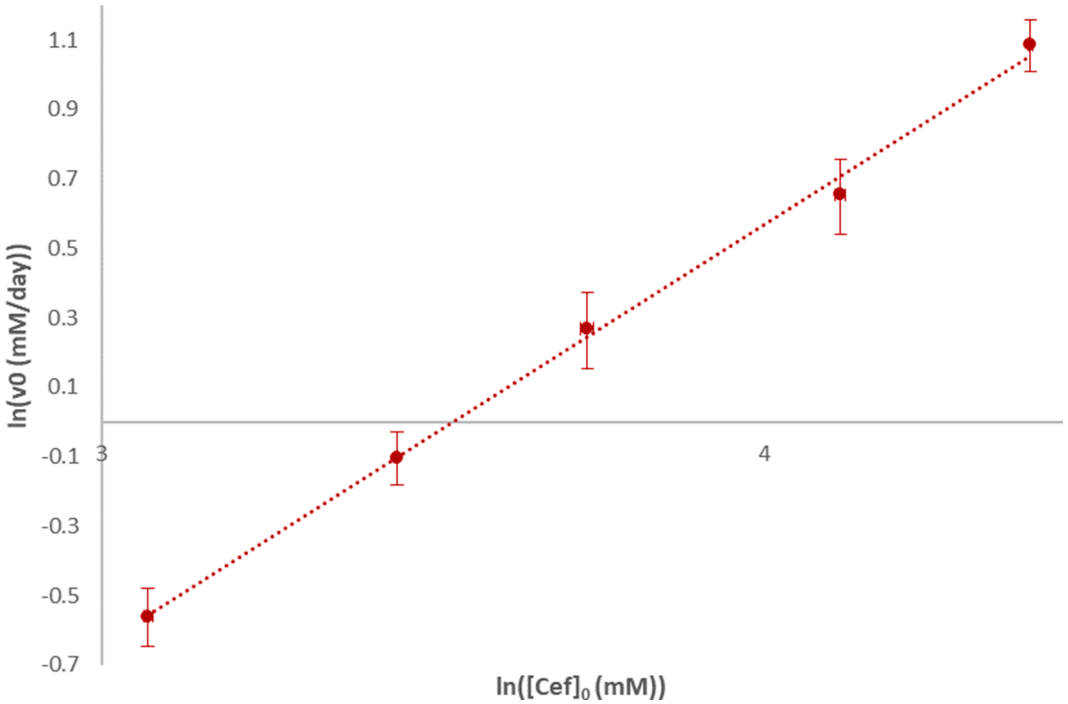

Fig. 13. Degradation rates of ceftriaxone from different initial concentrations, starting at pH 6.7 (experiments and sampling were each carried out in triplicate; error bars for the rate v0 are the standard error of the regression for each concentration; error bars for the initial Ceftriaxone concentration $[Cef]_0$ are at the 99.5% confidence level; the R^2 value is 0.997).

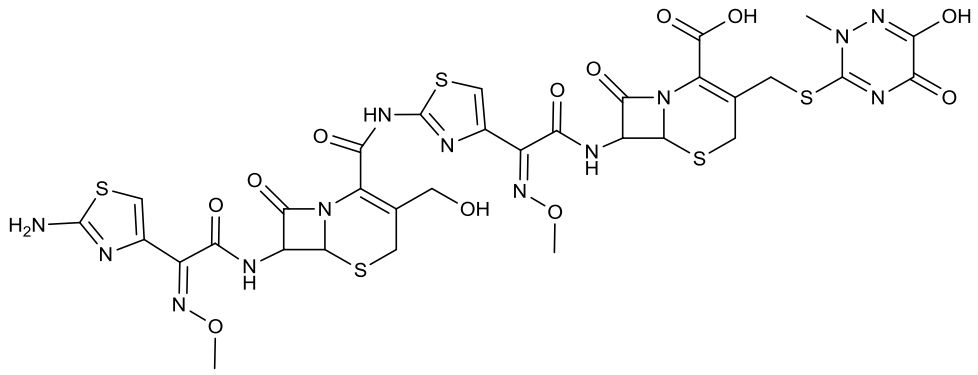

Fig. 14. A plausible structure for the Dimer impurity.

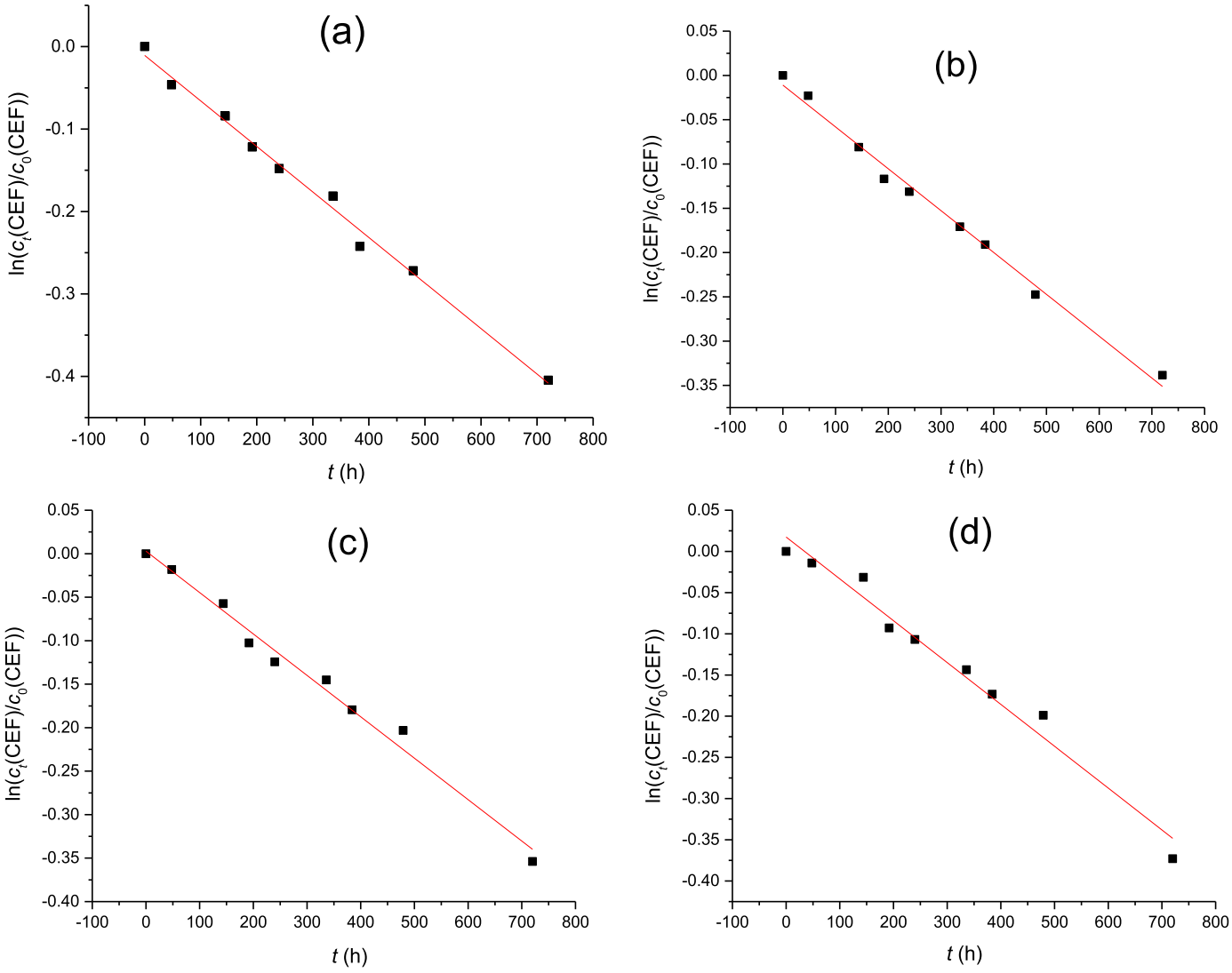

Fig. 15. CEF degradation in aqueous solvent containing 10% (a), 25% (b), 50% (c), and 75% (d) of D_2O at 25 °C processed by assuming first-order kinetics. CEF concentration was determined by quantitative ^1H NMR spectroscopy using the proton signal at 6.91 ppm integrated against DMAc as internal standard. $pH_0 = 6.8$, $c_0 = 0.036$ M; ■ experimental — calculated.

acid/base equilibriums, which offer the final product (P) with a cationic amine and two anionic carboxylates, yielding the total reaction free energy of $\Delta G_R = -4.8$ kcal mol^{-1}. To validate these results, let us mention that the stepwise character of this process agrees with earlier reports on similar systems in solution (East, 2018; Slebocka-Tilk et al., 2002), and was recently also confirmed as operative even for the enzymatic hydrolysis of β-lactams (Wei et al., 2021). Along these lines, our calculations for the concerted mechanism, which avoids the tetrahedral intermediate and allows the final product (P) in a single step, give a much higher barrier of $\Delta G^{\ddagger} = 47.0$ kcal mol^{-1}, thereby excluding it as

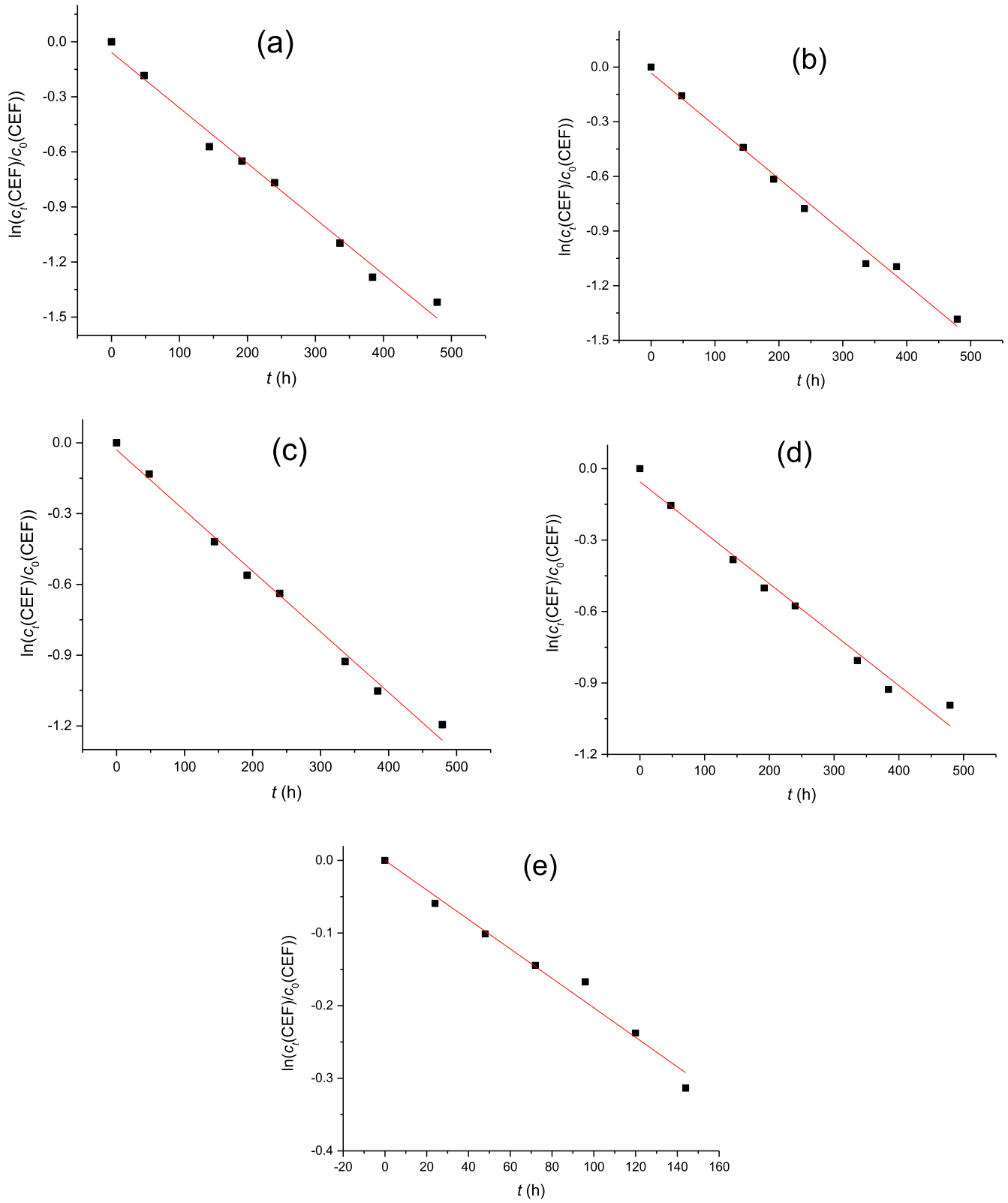

Fig. 16. CEF degradation in aqueous solvent containing 10% (a), 25% (b), 50% (c), 75% (d) and 100% (e) of D_2O at 40 °C processed by assuming first-order kinetics. CEF concentration was determined by quantitative ^1H NMR spectroscopy using the proton signal at 6.91 ppm integrated against DMAc as internal standard. pH_0 = 6.8, c_0 = 0.036 M; ■ experimental — calculated.

Table 2
Kinetic parameters for ceftriaxone degradation at various compositions of H_2O/D_2O solvent mixtures. $pH_0 = 6.8$.[a]

% D_2O	1000 × k(25 °C)(h^{-1})	1000 × k(40 °C) (h^{-1})
0	0.54(1)[b]	4.6(1)[b]
10	0.51(4)	4.1(1)
25	0.49(2)	4.0(1)
50	0.43(1)	3.4(1)
75	0.38(3)	2.74(8)
100	0.33(2)[b]	1.80(3)

[a] uncertainties of the last digits are expressed in parentheses as standard errors of the mean.
[b] value obtained by extrapolation of linear function k vs% D_2O.

viable. Finally, the obtained barrier for the most feasible stepwise route, $\Delta G^{\ddagger} = 27.5$ kcal mol^{-1}, agrees with results measured for similar systems (Mitchell et al., 2014) and with the value (26.8 kcal mol^{-1}) determined experimentally in this work by applying the Eyring equation. This points out the reliability of the computed value.

Given that the triazine protonation ($pK_a = 4.21$) occurs under conditions only slightly more acidic than those considered in our work, we found it necessary to investigate the feasibility of the β–lactam ring opening starting from the monoanionic CEF^- with unionized triazine, and evaluate the accessibility of this process at pH = 7 (Table S1). The distant nature of triazine from the β–lactam unit justifies its insignificance for the stability of the latter, seen in only markedly changed activation energy of $\Delta G^{\ddagger} = 27.8$ kcal mol^{-1}, which reveals two important aspects. Namely, the fact that the activation barrier shows practically no sensitivity towards this change in the CEF protonation form is found in excellent agreement with Mitchell et al. (2014), who reported an unchanged stability of three β-lactam antibiotics in the range 4 < pH < 7. In addition, knowing that at pH = 7, it requires 3.8 kcal mol^{-1} to allow the monoanionic CEF^-, increases the suchlike barrier to $\Delta G^{\ddagger} =$ 31.6 kcal mol^{-1}, which renders it much less feasible than the reaction with CEF^{2-}, and was not considered further. This, of course, must not be confused with a plethora of literature that advise the increased vulnerability of β–lactams in acidic media (Wan et al., 1980), yet only in those acidic enough that allow for the protonation of the β–lactam moiety. Knowing that pK_a values for simple lactams are typically below zero (Wan et al., 1980) helps interpret their enlarged instability with the

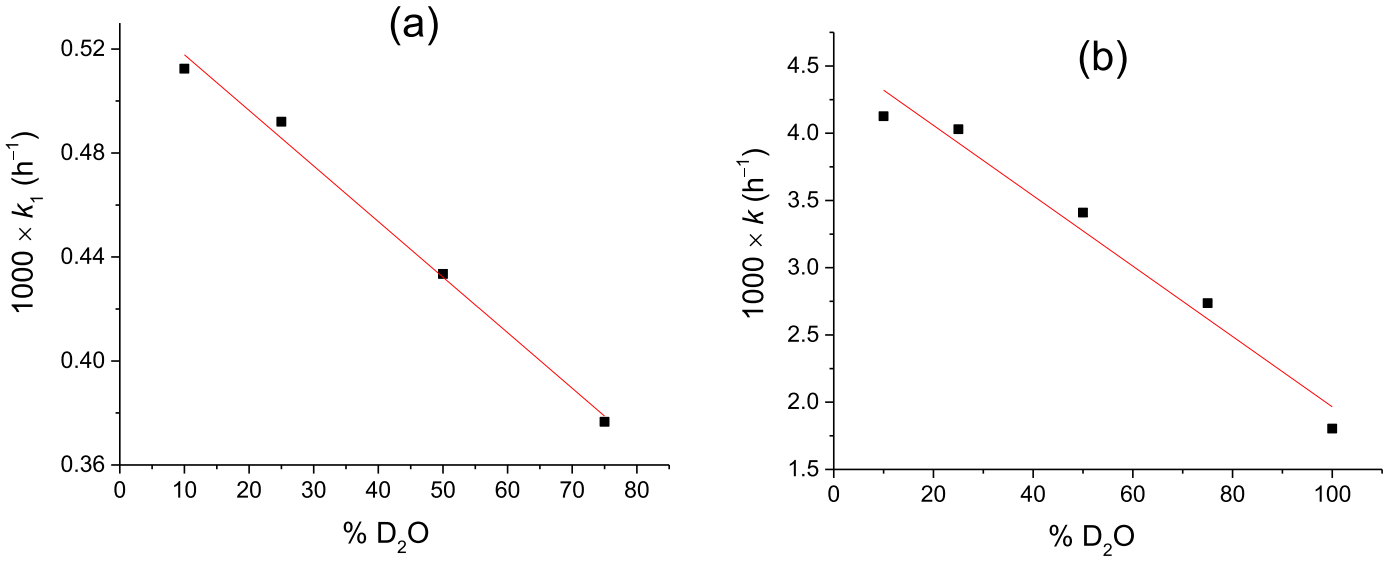

Fig. 17. Dependence of first-order rate constant for CEF degradation in H_2O/D_2O mixtures on solvent composition at 25 °C (a) and 40 °C (b). $pH_0 = 6.8$.

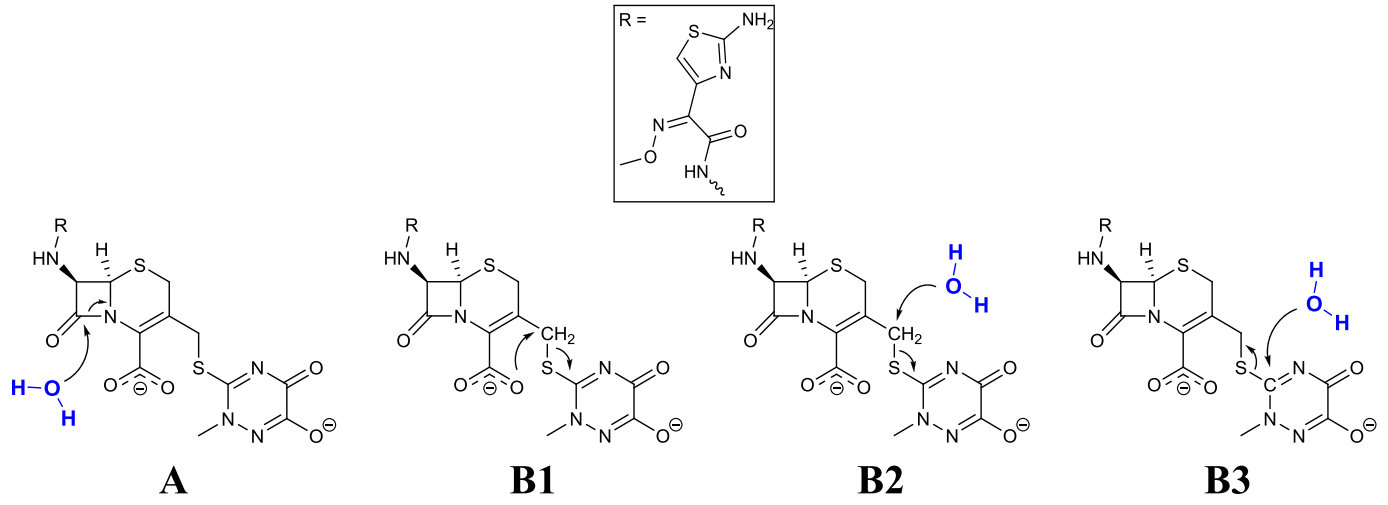

Fig. 18. Ceftriaxone degradation routes studied in this work, including the β-lactam ring opening (A) or the cleavage of the central C–S bond, the later proceeding either through the internal participation of the vicinal carboxylate (B1) or involving the nucleophilic substitution on either the alkyl (B2) or the ring (B3) carbon atom.

Table 3
The stability of different stationary points relative to the isolated reactants during the β–lactam ring opening in the dianionic ceftriaxone CEF^{2-} at pH = 7. The influence of Na^+ ions bound at different CEF sites on the reaction outcomes is presented in the last three columns. Data in shading indicate the rate-limiting activation barrier and the overall reaction thermodynamics. All values (in kcal mol^{-1}) are obtained through the (SMD)/M06–2X/6–31+G(d) model in water.

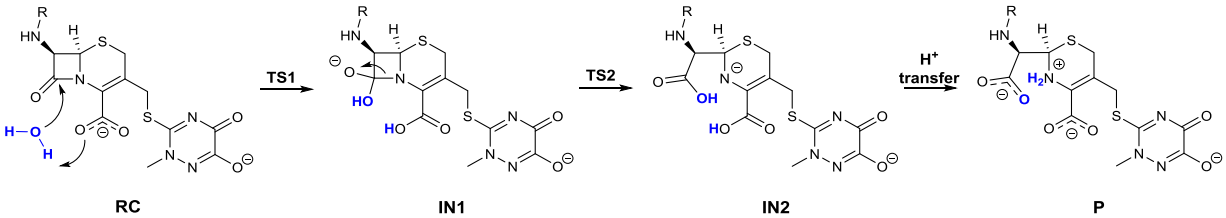

Conditions	pH = 7	$COO^-\cdots Na^+$	$CO_{\beta\text{-lactam}}\cdots Na^+$	$CO_{triazine}\cdots Na^+$
isolated reactants	0.0	0.0	0.0	0.0
RC	3.4	4.9	3.9	4.5
TS1	27.5	29.3	25.5	27.7
IN1	13.2	20.4	5.7	13.2
TS2	15.9	22.2	11.8	16.6
IN2	11.3	11.1	2.9	5.5
P	−4.8	−4.8	−4.8	−4.8

subsequent addition of the sulfuric acid, which passes through a maximum in the region 20–25% H_2SO_4 (Wan et al., 1980). In our case, no external acid was added which makes the described process for the anionic CEF^- irrelevant for the current discussion.

On the other hand, CEF contains no acidic sites that are accessible upon a moderate pH increase, yet this brings about an excess of OH^- anions having a much larger nucleophilicity over unionized water. This will significantly stimulate the degradation (Table S1), despite more energy required to form the reactive complex (RC) with OH^-, given its more favorable solvation relative to H_2O. Yet, the attack on the β–lactam carbon requires only $\Delta G^{\ddagger} = 16.1$ kcal mol^{-1} in total, which represents a remarkable catalytic effect of 8-orders of magnitude. In that case, even the formed tetrahedral intermediate (IN1) experiences some stability over the isolated reactants (–2.6 kcal mol^{-1}), while its successive β–lactam ring opening is again efficient and leads to a further downhill product (IN2) at –7.6 kcal mol^{-1}. Following an analogous H^+-transfer reactions, the final product (P) is formed in a highly exergonic fashion, $\Delta G_R = -37.9$ kcal mol^{-1}. This indicates that exceedingly basic conditions should be avoided if a prolonged CEF stability is required, which firmly agrees with Mitchell et al. (2014) who studied β–lactam degradation in three antibiotics and its pH dependence, but reported results only up to pH = 9, where the reactions proceeded most rapidly, while more basic conditions led to reactions too efficient to allow for a proper analytical characterization of degradation products.

In concluding this section, at pH = 7, the β-lactam hydrolysis involves three steps, (i) the rate-limiting nucleophilic attack of water onto the β-lactam amide carbon concerted with the proton transfer onto the vicinal carboxylate, which offers a tetrahedral intermediate, (ii) the opening of the β-lactam ring, which generates a negative charge on the liberated amine, and (iii) several acid/base proton transfer equilibria that yield the final product. Its feasibility under neutral conditions is evident in the computed values of $\Delta G^{\ddagger} = 27.5$ kcal mol^{-1} and $\Delta G_R = -4.8$ kcal mol^{-1}, and is responsible for a variety of degradation products with a disintegrated β-lactam ring.

2.6. Cleavage of the carbon–sulfur bond

The degradation of CEF at a linker connecting triazine with the rest of the structure appears more complex, given a variety of different degradation products originating from the processes likely occurring at that site. Identification of products containing a lactone moiety clearly indicates a participation of the negatively charged carboxylate, while the recognition of a liberated triazine, having either –OH or –SH groups at the C-2position, suggests that external nucleophiles could induce an S_N2 substitution reaction at the corresponding either alkyl or ring carbon atoms, which warrants their separate considerations.

The calculated homolytic bond dissociation energies (BDEs) of central C–S bonds involving the alkyl and ring carbons are 32.5 and 65.7 kcal mol^{-1}, respectively. Both are significantly lower than, for example, 73 kcal mol^{-1} experimentally measured in CH_3–SH (Mackle and McClean, 1962), which already hints at their instability. Under neutral conditions, the nearby carboxylate appears like an adequate nucleophile to initiate the reaction, at least from the C(alkyl) site, because of its non-optimal distance and orientation from the ring carbon. This reaction can proceed in two ways, either concertedly or in a stepwise fashion (Table 4).

Interestingly, at pH = 7, the stepwise mechanism, that is the cleavage of the C(alkyl)–S bond without the participation of a carboxylate, proceeds through a barrier which is by 4.2 kcal mol^{-1} lower from that in the concerted alternative. Yet, if offers a very unstable methylene intermediate (IN1), which can be subsequently attacked by the solvent water. Although this requires only 10.3 kcal mol−1 in the activation energy, the high energy of the reacting intermediate leads to the increase in the overall barrier to $\Delta G^{\ddagger} = 31.5$ kcal mol^{-1}, making it comparable, yet slightly less feasible than in the concerted pathway. Still, it allows a stable alcohol (IN2), which represents a prerequisite for the matching lactone in this scenario. The latter sequence is unable to occur from a neutral alcohol, with OH^- being a poor leaving group, and leading to a high barrier of $\Delta G^{\ddagger} = 47.2$ kcal mol^{-1} from IN2. Instead a prior alcohol protonation must occur, which, at pH = 7, demands 12.6 kcal mol^{-1}, as evaluated from $pK_a = -2.26$ for the ethanol protonation (Chrisment and Delpuech, 1977) and additional 8.8 kcal mol^{-1} for the transition state, leading to a very stable lactone as a final product (P). Although feasible, and likely responsible for the eventual alcohol-type degradation products (IN2), the presented stepwise scenario is somewhat preceded by a concerted pathway (Table 4), where the lactone is formed in a single

Table 4
The stability of different stationary points relative to the isolated reactants during the C(alkyl)–S bond cleavage in the dianionic ceftriaxone CEF^{2-} at pH = 7. The influence of Na^+ ions bound at different CEF sites on the reaction outcomes is presented in the last three columns. Data in shading indicate the rate-limiting activation barrier and the overall reaction thermodynamics. All values (in kcal mol^{-1}) are obtained through the (SMD)/M06–2X/6–31+G(d) model in water.

CONCERTED MECHANISM

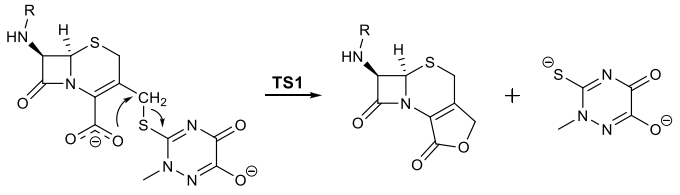

CEF P

Conditions	pH = 7	$COO^-\cdots Na^+$	$CO_{\beta\text{-lactam}}\cdots Na^+$	$CO_{triazine}\cdots Na^+$
CEF	0.0	0.0	0.0	0.0
TS1	31.1	35.5	30.0	29.9
isolated products	−9.5	−9.5	−9.5	−9.5

STEPWISE MECHANISM

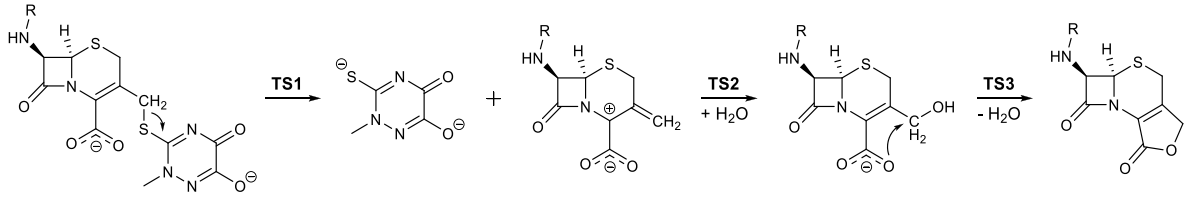

CEF IN1 IN2 P

Conditions	pH = 7	$COO^-\cdots Na^+$	$CO_{\beta\text{-lactam}}\cdots Na^+$	$CO_{triazine}\cdots Na^+$
CEF	0.0	0.0	0.0	0.0
TS1	26.9	30.5	26.2	26.6
IN1	21.2	27.0	21.6	19.8
TS2	31.5	36.1	30.1	30.1
IN2	2.4	12.2	0.4	1.0
TS3	21.4	33.9	20.4	20.0
isolated products	–9.5	–9.5	–9.5	–9.5

step through the barrier of $\Delta G^{\ddagger} = 31.1$ kcal mol^{-1}. The obtained barrier difference of 0.4 kcal mol^{-1} suggests a two times faster process, which likely dominates for the lactone formation. We note in passing that the calculated exergonicity of $\Delta G_R = -9.5$ kcal mol^{-1} includes a contribution for the thiolate protonation in the liberated triazine part. Namely, thiols are weak acids, so at pH = 7 they are typically unionized, which led us to include an estimated –5.0 kcal mol^{-1} to the reaction free energy, based on the $pK_a = 10.69$ for the cyclohexanethiol deprotonation (Zhang, 2012). Even more importantly, the fact that, during the reaction, the triazine fragment is liberated with an anionic thiolate, which consumes protons and is spontaneously converted into an unionized thiol, helps explaining an observed slight initial increase in the pH conditions in the performed experiments (Table 3). We feel this notion additionally confirms both the mechanistic proposal and the calculated reaction parameters presented in the text.

Unlike the β–lactam hydrolysis, one could expect a notable effect of the triazine protonation on the reaction outcomes here. Indeed, starting from the monoanionic CEF^- (Table S2), the concerted pathway requires $\Delta G^{\ddagger} = 28.4$ kcal mol^{-1} to cleave the C–S bond, yet when 3.8 kcal mol^{-1} is added to allow CEF^- at pH = 7, the increased barrier of $\Delta G^{\ddagger} = 32.2$ kcal mol^{-1} suggests this as an unlikely route for the lactone formation. In contrast, a stepwise reaction becomes relatively efficient in CEF^- with $\Delta G^{\ddagger} = 22.5$ kcal mol^{-1}, which, even when the mentioned triazine protonation correction is applied, offers a reduced barrier of $\Delta G^{\ddagger} = 26.3$ kcal mol^{-1} that goes below the concerted mechanism. Yet, since this does not represent the rate-limiting step of the entire transformation, the latter residing in the addition of water onto the methylene intermediate that is identical in both pathways, we conclude that the system will not utilize the triazine protonation to afford the lactone-type products. In contrast, given that OH^- anions can more readily add to the methylene intermediate (IN1), an excess of the former again facilitates the conversion by reducing the barrier of this step to $\Delta G^{\ddagger} = 1.1$ kcal mol^{-1}

(Table S2), thereby making the pathway towards IN1 as rate-limiting with $\Delta G^{\ddagger} = 26.9$ kcal mol^{-1}, which once more advises ruining conditions for the CEF stability. Still, we have to emphasize that the IN1 production with CEF^{-}, even at pH = 7 where $\Delta G^{\ddagger} = 26.3$ kcal mol^{-1}, turned out to be the most feasible initial process for the CEF degradation. Given its high instability and a pronounced reactivity, we feel this intermediate is likely the starting point of several other more complex degradation products, even the dimeric impurity 949 identified here. Specifically, a subsequent attack of another CEF molecule onto the methylene site in IN1, would offer a compound with a molecular mass corresponding to impurity 949. Given a large number of potential CEF sites that could engage in such dimerization, and without a precise experimental knowledge of its molecular structure, this process was not studied in any detail, but we feel this opens a viable route towards impurity 949, and its more accurate identification remains a challenge for future experiments.

Lastly, we inspected the tendency of external nucleophiles to cleave either of the studied C–S bonds (Table S3). Starting with the unionized water at pH = 7, relevant for our work, the attack on the alkyl carbon proceeds with the concerted H^{+}-transfer to the vicinal carboxylate, yet the reaction requires a high kinetic barrier, $\Delta G^{\ddagger} = 38.4$ kcal mol^{-1}, and is only moderately exergonic, $\Delta G_R = -2.9$ kcal mol^{-1}. Alternatively, when the approach involves the ring carbon, it is assisted with the triazine anionic nitrogen, yet it is even less feasible, seen in $\Delta G^{\ddagger} = 53.6$ and $\Delta G_R = -0.8$ kcal mol^{-1}, which eliminate both processes as likely. The latter holds even when H_2O is considered with the unionized triazine in CEF^{-} in both pathways (Table S3). On the contrary, nucleophilic OH^{-} anions again turn out as more reactive. Still, their catalytic rate-enhancement for the S_N2 liberation of triazine at the alkyl carbon assumes 6-orders of magnitude, or a reduced barrier of 8.0 kcal mol^{-1} relative to neutral conditions with H_2O, being lower than calculated for the β–lactam ring opening. On the other hand, OH^{-} are even able to displace the sulfur atom from the triazine ring, with calculated parameters $\Delta G^{\ddagger} = 18.8$ and $\Delta G_R = -25.0$ kcal mol^{-1}, which is likely responsible for the liberated triazine product containing 2-hydroxy moiety instead of its 2-merkapto analogue, provided that reaction conditions allow this transformation.

In summary, we conclude that under investigated conditions (pH = 7), the most likely CEF degradation route focused on the central C–S linker involves the nucleophilic attack of the vicinal carboxylate on the alkyl carbon atom, which liberates the triazine fragment with a concerted formation of lactone. This route slightly dominates over the stepwise process that proceeds through the unstable methylene intermediate, which subsequently gives a lactone through the alcohol intermediate. Knowing that the latter scenario occurs only 2 times slower than the concerted route justifies their coexistence and helps interpreting the formation of suchlike alcohol products reported in the literature. More importantly, the calculated $\Delta G^{\ddagger} = 31.1$ and $\Delta G_R = -9.5$ kcal mol^{-1} for the most feasible concerted pathway strongly indicate a competition with the β–lactam hydrolysis. In other words, the described C–S bond cleavage requires more time (increased barrier by 3.6 kcal mol^{-1}), but is thermodynamically more favored (increased exergonicity by –4.5 kcal mol−1). In contrast, the β–lactam hydrolysis will offer degradation products faster, yet in lower quantities once both processes reach the equilibrium. This could, for example, imply that during very early detections of degradation products, the solution might not even contain lactone- or alcohol-type compounds without the triazine fragment, which needs to be considered if a proper relationship between identified products and reactions leading to their formation is to be drawn. Of course, although one could argue that, perhaps, initially the β–lactam ring opening dominates and is the exclusive degradation route, while its products allow a more favorable subsequent C–S bond cleavage, we feel this is unlikely due to a distant nature of both fragments, which agrees with experimental conclusions (Zając and Muszalska, 1998). If operative, this could likely modify only the thermodynamic aspects of the C–S bond cleavage, not the kinetic requirements, which is why this was not investigated in detail. Instead, we can confidently conclude that within the time-frame of the performed experiments, both routes compete for the CEF degradation and are jointly responsible for the detected products. Lastly, in the context of the evaluated solvent kinetic isotope effect, one needs to observe an opposing solvent outcome on both processes. While, during the β–lactam hydrolysis, the solvent directly participates in the rate-limiting tetrahedral intermediate formation, thus a significant SKIE could be expected, the C–S bond cleavage, in the most favorable concerted scenario, experiences a much lower solvent impact, and a much inferior (or even inverse) SKIE will be exerted. To validate this notion, let us mention that the SKIE of 1.84 ± 0.09 obtained here is rather large, yet significantly smaller than, for example, 2.9 measured for the spontaneous hydrolysis of acetic anhydride (El Seoud et al., 1997) or 2.5 for the formamide hydrolysis at pH = 7 (Slebocka-Tilk et al., 2002), where only the hydrolytic reaction is possible. Even more so, the latter work reported an inverse SKIE of 0.77 for the base-catalyzed reaction at high [OH^{-}] (Slebocka-Tilk et al., 2002), which is reasonable as, according to our mechanistic proposal (Table 3), it proceeds without the cleavage of the O–H/D bond in the rate-limiting step, which excludes significant positive SKIE effects. This hints at an interesting proposal that the SKIE observed in our experiments could potentially result as a compromise between a nominally much larger effect for the β–lactam hydrolysis and an inverse effect for the C–S bond cleavage. Although this might represent a quantitative oversimplification of the effects occurring in solution, in qualitative terms, we strongly believe these examples firmly confirm that a combination of both identified degradation processes is operative during CEF degradation.

2.7. The effect of the solution components on degradation reactions

Under neutral conditions, CEF is a dianion and is introduced in the aqueous solution as its disodium salt. This implies that experimentally characterized systems contain two equivalents of Na^{+} ions, which can potentially interact with CEF and interfere with degradation processes. This is why we have repeated mechanistic calculations for both feasible degradation routes at pH = 7 with Na^{+} ions bound to three prominent CEF sites: (i) anionic carboxylate, (ii) anionic triazine, and (iii) β–lactam amide oxygen. The results are provided in Tables 3 and 4, while the changed kinetic parameters following CEF•••Na^{+} interactions will help to interpret the results of the molecular dynamics simulations and rationalize the effect of replacing H_2O with D_2O on the CEF stability.

Preceding DFT analysis clearly underlined a significant role of the free carboxylate on both degradation pathways. While during the β–lactam hydrolysis, it assists in the rate limiting addition of water onto the amide carbon through the concerted H^{+}-abstraction from the solvent nucleophile, its role in the C–S cleavage is even larger as it initiates the reaction by attacking the alkyl carbon atom. Both aspects are facilitated by its anionic character, which either makes it a good base or a good nucleophile, respectively. Therefore, it is not surprising that once the solution interactions between carboxylate and Na^{+} ions are afforded, it will slow down both CEF degradation processes because of a reduced amount of the negative charge available for the reaction. This is evident in 1.8 kcal mol−1 higher barrier for the β–lactam hydrolysis and as much as 4.4 kcal mol^{-1} for the C–S cleavage, which will clearly improve the CEF stability. In contrast, any Na^{+} interactions with the β–lactam ring will activate it for the hydrolysis, analogously to the β–lactam protonation in exceedingly acidic solutions (Wan et al., 1980) seen in 2.0 kcal mol^{-1} barrier reduction, while this effect on the C–S cleavage is, expectedly, less pronounced. On the other hand, the same logic applies to the Na^{+}•••triazine interactions, which facilitate triazine liberation by reducing the barrier by 1.2 kcal mol^{-1}, while their effect on the β–lactam hydrolysis is negligible. Therefore, as the most significant outcome, we can conclude that any considerable interactions with the anionic carboxylate will reduce CEF degradation, while those with the other two sites, the β–lactam ring and the triazine unit, will facilitate the product

formation. Although this analysis was based on considering the Na^+ ions present in solution, in a broader sense, this also illustrates the effects of other solution components that would be able to interact with CEF, solvent molecules at first, where an analogous analysis would reveal identical qualitative trends. The latter clearly also holds for the actual protonation of these CEF sites, and this notion helps us rationalize another very interesting aspect. Namely, it might appear confusing at first that Zając and Muszalska (1998) observed no open β–lactam ring degradation products in CEF when experiments were performed in the exceedingly acidic environment at pH = 0.42, where only products originating from the C–S bond rupture were detected, which might contradict the already mentioned excessive hydrolytic instability of lactams in H_2SO_4 (Wan et al., 1980). To interpret that, we must realize that, obviously, there will almost certainly exist a particular pH range, where both the carboxylic unit and the β–lactam ring will be unionized. According to our DFT analysis, such a combination of solution conditions will hinder the β–lactam ring opening and promote the C–S bond cleavage. The pH value of 0.42 utilized by Zajac and Muszalska seems to fall precisely in that range, knowing that the acidity of carboxylic group in CEF is $pK_a = 2.37$, and that pK_a values for simple lactams are typically below zero (Wan et al., 1980), which is easily achieved by H_2SO_4 having pK_a around –4 in the aqueous solution (Benoit and Buisson, 1973).

2.8. Molecular dynamics simulations in H_2O and D_2O solvents

We carried out molecular dynamics simulations of CEF disodium within simulations boxes containing explicit H_2O or D_2O molecules in order to inspect how both solvents are affecting CEF in solution and a range of intra- and intermolecular interactions it can undertake.

The first thing we analyzed was the overall solvation taking three most significant CEF sites, anionic carboxylate, anionic triazine, and β–lactam amide oxygen, as illustrative examples. Although an increased carboxylate solvation following a solvent change will enhance the CEF stability, while that of the other two site could lead to its increased degradability, it turned out that both solvents are identically interacting with CEF during simulations (Fig. S1), and that there are no notable differences that could help interpreting altered CEF stabilities. Yet, the obtained RDF displays point to several interesting conclusions. The approach of solvent towards all three sites is equally successful, as all three graphs have the first peak at the relevant O(solvent)•••O(CEF) distances slightly below 3 Å, which indicate rather strong interactions. Still, for the β–lactam moiety, these are significantly less frequent than with the remaining two sites, evidently because of its uncharged nature relative to the other two moieties. However, an almost perfect overlap of all three RDF curves for both H_2O and D_2O indicates that solvent, on its own, does not provide any significant contribution towards the modified CEF stability. Like so, we observed no differences in the CEF conformational preference in either solvent, as representative structures in both cases are the same and reveal no particular intramolecular contacts (Fig. S2).

The situation with the CEF•••Na^+ interactions is considerably different (Fig. 19). In H_2O, Na^+ ions show a moderate tendency towards all three CEF sites. Yet, surprisingly, it is highest towards the triazine unit, where the relevant Na^+•••O contacts occur in 3.8% of structures during simulations (Fig. S3). This represents an almost 50% increase from the number of analogous contacts with carboxylate, observed in 2.6% structures. Lastly, interactions with the uncharged β–lactam are least frequent and are taking place in 1.2% of structures, being identical in both environments, thereby not making any difference among solvents. Although all CEF•••Na^+ interactions are, in general, not persistent and are only rarely happening in solution, the demonstrated relative preference of Na^+ ions to be located around triazine over carboxylate is assisting in the CEF degradation. Namely, according to our DFT analysis, it is precisely the Na^+•••triazine contacts that facilitate the cleavage of the central C–S bond (Table 4), which agrees with experimental results presented here. In contrast, when H_2O is replaced with D_2O, two effect operate in synergy towards improving the CEF stability, namely (i) the frequency of favorable interactions with carboxylate increases 2,5 times, while (ii) the occurrence of the unfavorable contacts with triazine is reduced almost 4 times, assuming a value even lower than that for the matching interactions with the β–lactam ring. Therefore, such an illustrative insight helps in rationalizing an increased stability of CEF in D_2O, which is, apart from the obvious effect of slowing down the degradation processes where the solvent molecules are directly participating, also based on improving the electrostatic interactions with CEF sites that are favorable for its stability, while reducing those that help in its degradation.

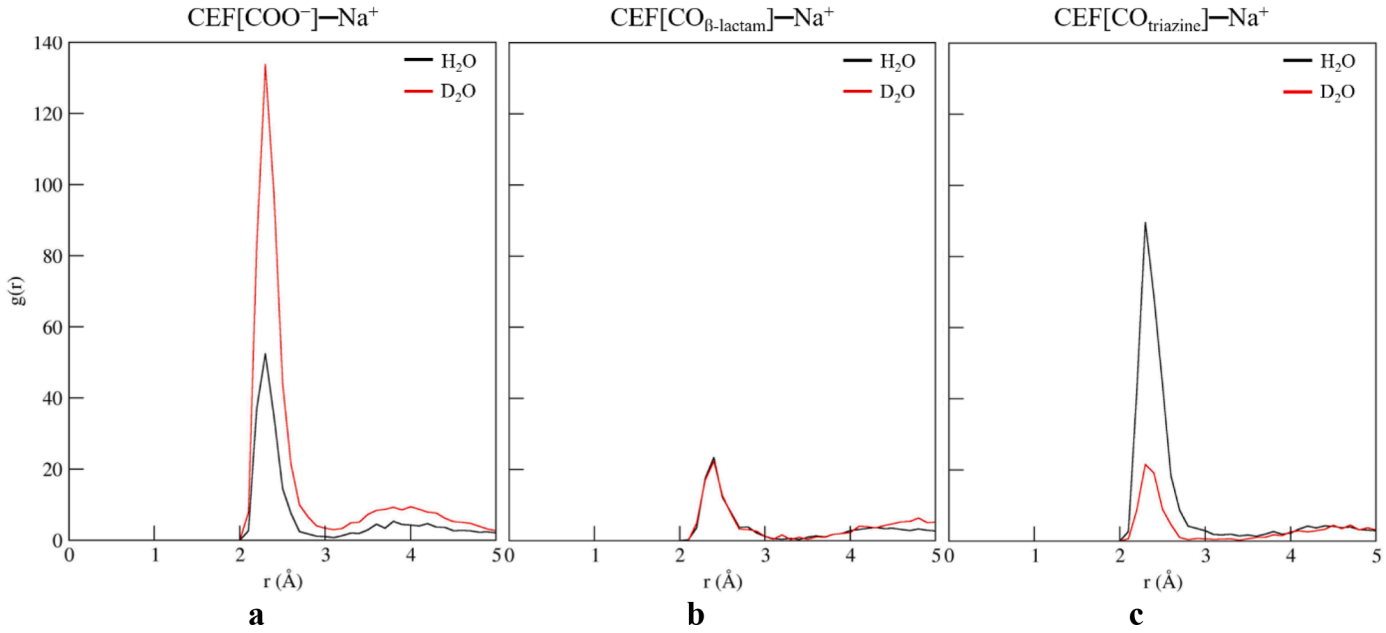

Fig. 19. RDF displays considering the approach of Na^+ ions onto the (a) carboxylate oxygen atoms, (b) β–lactam amide oxygen atom, and (c) triazine oxygen atom in the dianionic **CEF^{2-}** at pH = 7 in H_2O (in black) and D_2O (in red) solutions following 100 ns of the corresponding molecular dynamics simulations.

3. Methods

Ceftriaxone Sodium was supplied by Kyongbo Pharmaceuticals, Water for Injection from BBraun, Ultrapure water was produced by MiliQ purification system, deuterium oxide (NMR Suitable) from Merck and sodium deuteroxide from Merck (NMR suitable). Ceftriaxone Sodium reference standard was sourced from Ph.Eur. Phosphate buffer (Sodium Phosphate Monobasic) were purchased from Fluka, while phosphoric acid was obtained from VWR (for HPLC grade). Supelco Titan C18 100 × 2.1 mm; 1.9 μm column was supplied by Sigma Aldrich.

3.1. Preparation of ceftriaxone compositions

A predefined solvent volume (Water for Injection (WFI), predefined mixture of WFI and deuterated water (D_2O), or just D_2O) at the temperature of 15 °C-25 °C was collected in a laboratory glass. The dispensed quantity of ceftriaxone sodium was added into the WFI to achieve the final ceftriaxone concentration of 20 mg mL^{-1} and the solution was mixed until the substance was dissolved (clear solution without visible particles was obtained). Solvent at the temperature in the range of 15 °C–25 °C was added to make the solution up to the prescribed volume to give the concentration of 20 mg mL^{-1} of ceftriaxone, and the solution was stirred for no less than 1 min. The solution was then filtered through a 0.2 μm filter and filled into glass vials, stoppered with rubber stoppers and sealed with aluminum seals. Vials were either analyzed at the start for predefined parameters or loaded at stress/stability testing and analyzed as per defined schedule for agreed parameters.

3.2. HPLC analysis

Chromatographic analysis of ceftriaxone assay and predetermined impurities was performed using a C18 Supelco Titan 100 × 2.1 mm; 1.9 μm column. Mobile phases consisted of 10 mM phosphate buffer with the pH adjusted to 2.3 with phosphoric acid (mobile phase A), and 50% 10 mM phosphate buffer and 50% acetonitrile (mobile phase B). Gradient elution was employed as described in Table 5 below. Injection volume was equal to 3 μL. Column temperature was adjusted to 35 °C, and flow was set to 0.400 mL/min. Detection was performed at 254 nm.

The targeted concentration of ceftriaxone (free base) in *Sample* and *Standard* solutions was about 0.08 mg mL^{-1}. The standard solution was prepared by weighing and dissolving 4.000–5.000 mg of ceftriaxone sodium reference standard in a 50 mL volumetric flask with MilliQ water. The sample solution was prepared in the following manner: about 0.4 mL of sample solution was weighed into a 100 mL volumetric flask and diluted to volume with MilliQ water. The density of the composition was determined. The sample and standard solutions were prepared in duplicate.

Response factor (RF) was calculated as means of calibration of the system and then used to calculate ceftriaxone amount in the sample. Calculation of the detector response factor (RF) of ceftriaxone in standard solutions was performed using the following equation:

RF = Area of ceftriaxone peak / concentration of ceftriaxone free base in standard solution

Ceftriaxone assay calculation was performed in the following manner:

$$\frac{Area of Cef peak in sample solution * Density of formulation\left(\frac{g}{mL}\right) * 100(mL) * 100\%}{Average RF of standard solution * weight of sample(g) * 20}$$

Relative standard deviation (RSD) of standard response factors was calculated (and the requirement was NMT 1%), and recovery of assay results of two sample preparations should be between 0.985 and 1.015.

Stability of prepared ceftriaxone samples was expressed as drop of ceftriaxone assay measured at specific time point compared to ceftriaxone assay measured at the time of preparation. Also, increase of predefined degradation products were monitored during stability testing during predefined period at predefined temperature conditions.

Table 5
Composition of the mobile phase during chromatography experiments (gradient elution).

Time (min)	% A	% B
0	98	2
10	80	20
12.5	77	23
30	0	100
31	98	2
36	98	2

3.3. LC-MS (MS/M) analysis

For LC-MS anaysis the same chromatographic conditions were used as for HPLC analysis except the phosphate buffer was replaced with 0.3% Formic Acid. Q-TOF (Quadropole Time of flight) MS instrument was used equipped with Electrospray ionization source (ESI).

3.4. Kinetic isotope effect (KIE) study

For each experiment, Ultrapure grade water (10.000 ± 0.001 g) was weighed into a glass tube, and to this was added the ceftriaxone sodium salt (200.0 ± 0.1 mg), giving a concentration of approximately 20 mg mL^{-1}. The mixture was capped and shaken to ensure that all of the solid had dissolved. Samples for the $t = 0$ timepoint were then taken. A 200 μL pipette was used to transfer 400 μL of the solution into a 100 mL volumetric flask. The volume was made up to 100 mL with MilliQ water and the solution was vigorously shaken. Approximately 1 mL of this was transferred to an HPLC vial and the sample was analyzed by HPLC (the carousel temperature was maintained at 5 °C). Once the reactions had been set-up and the $t = 0$ sampling complete, the tubes were covered in aluminum foil, and the temperature was maintained at 25 °C. Sampling was carried out for 7 days at approximately 24 h intervals. The samples were analyzed by HPLC using the method described above. A 9-point calibration curve was run just prior to analyzing the samples. For consistency, integration of the ceftriaxone peak was done manually using fixed time points before and after the time of the maximum peak height. This was then converted into a mM concentration value, which was plotted against time. As water is in a large excess, the kinetics effectively becomes zero order in water. Also, as we are studying the degradation of Ceftriaxone within the first 10% of reactivity, we are considering initial rates and therefore should be able to model this data as a straight line. Error bars are at the 99.5% confidence level and were calculated using the Excel software. The equation and R^2 value for the trendline are calculated by Excel and under these conditions the k value (rate constant) for the reaction is equal to the gradient of the slope. In Excel, linear regression analysis was used to calculate the standard error in the slope and the intercept, which was used to provide the degree of uncertainty in the reported values for the number of days to 10% degradation, as well as the k value and the KIE.

For the KIE study at pH 7.5, just prior to taking the $t = 0$ HPLC samples, a 0.1 M solution of sodium hydroxide in Ultrapure water was added to the experiments in Ultrapure water until the pH was 7.50 ± 0.06. For the comparative experiments in deuterium oxide, the same volume of a 0.1 M solution of sodium deuteroxide in deuterium oxide was added.

3.5. Reaction order study

For each experiment, Ultrapure grade water (10.000 ± 0.001 g) was weighed into a glass tube, and to this was added the ceftriaxone sodium salt (200.0 ± 0.1 mg, 300.0 ± 0.1 mg, 400.0 ± 0.1 mg, 600.0 ± 0.1 mg, or 800.0 ± 0.1 mg). The mixture was capped and shaken to ensure that

all of the solid had dissolved. Samples for the $t = 0$ timepoint were then taken. A 200 μL pipette was used to transfer 400 μL, 300 μL, 200 μL, 150 μL or 100 μL (corresponding to the 200, 300, 400, 600 and 800 mg experiments) of the solution into a 100 mL volumetric flask. The volume was made up to 100 mL with MilliQ water and the solution was vigorously shaken. Approximately 1 mL of this was transferred to an HPLC vial and the sample was analyzed by HPLC (the carousel temperature was maintained at 5 °C). Once the reactions had been set-up and the $t = 0$ sampling complete, the tubes were covered in aluminum foil, and the temperature was maintained at 25 °C. Sampling was carried out for 5 days at approximately 24 h intervals.

The samples were analyzed by HPLC using the method described above. A 9-point calibration curve was run just prior to analyzing the samples. For consistency, integration of the ceftriaxone peak was done manually using fixed time points before and after the time of the maximum peak height. The μg/mL concentration in the HPLC vials was converted to mg mL^{-1} concentrations for the reactions themselves, using the weighed values for the water and ceftriaxone to adjust accordingly. This was then converted into a mM concentration value, which was plotted against time. As water is in a large excess, the kinetics effectively becomes zero order in water. Also, as we are studying the degradation of ceftriaxone within the first 10% of reactivity, we are considering initial rates and therefore should be able to model this data as a straight line. Error bars are at the 99.5% confidence level and were calculated using Excel. The equation and R^2 value for the trendlines are calculated by Excel and linear regression analysis was used to calculate the standard error in the slopes and the intercepts.

3.6. NMR study

The effect of H_2O/D_2O ratio on the ceftriaxone degradation kinetics was investigated by means of ^1H NMR spectroscopy at 25 and 40 °C. For that purpose, the solvents containing dimethyl acetamide (DMAc, $\gamma = 1.5$ mg mL^{-1}) as internal standard were prepared. The ceftriaxone solutions ($\gamma = 20$ mg mL^{-1}) were prepared by dissolving the appropriate amount of solid in 3 mL of solvent and the pH was adjusted to 6.8 with NaOH(aq). Solutions were transferred into NMR tubes and thermostated. The spectra of ceftriaxone in the above-mentioned media were monitored over time by means of Bruker Avance 400 spectrometer. The integrals of proton signals at 6.9 and 5.8 ppm were chosen for quantitative analysis of NMR data. The degradation percentage of CEF was calculated by subtracting the relative integral of signal at certain time ($I(t)$) from its value at the beginning (I_0) and dividing the obtained value by I_0.

The spectra were processed and integrated by means of MestReNova program package, whereas Origin 7.5. and Excel were used for data processing, statistical evaluation and presentation.

3.7. Computational details

3.7.1. Molecular dynamics simulations

MD simulations were carried out with GROMACS 2020.6 (Abraham et al., 2015) for 100 ns which corresponds to a total number of 50.000 frames, employing periodic boundary conditions in all directions. Ceftriaxone was located in the center of a 5.0 nm x 5.0 nm x 5.0 nm rectangular box and solvated with around 4.030 TIP3P H_2O water molecules, while 2 Na^+ ions were added to keep the overall charge of the simulation box neutral. The equations of motion were integrated with the time steps of 2 fs. The buffered Verlet neighbor list was used to evaluate the Lennard-Jones (6,12) interactions up to a distance cut off of 1.0 nm. Long-range electrostatic interactions were treated by the particle-mesh Ewald algorithm (Darden et al., 1993) with a 1.0 nm distance to switch between real and reciprocal space and a 0.12 nm grid spacing. The temperature of the system was kept at 298.15 K using the velocity rescaling thermostat of Bussi and co-workers (Bussi et al., 2007) with a coupling time constant of 1.0 ps, while a constant 1 bar pressure was achieved through the isotropic pressure coupling with the Parrinello-Rahman barostat (Parrinello and Rahman, 1981), with a 5 ps coupling time constant and a compressibility for water of $4.5 \cdot 10^{-5}$ bar^{-1}. The same setup was employed for D_2O solution simulations, where solvent D_2O molecules were modeled with the TIP3P-HW force field (Linse and Hub, 2021), which very efficiently captures the modulations of the mass, electron densities, heat of vaporization, diffusion coefficient, and structure relative to light water.

3.7.2. Quantum-chemical calculations

The starting points of the quantum-chemical calculations were the representative structures of ceftriaxone extracted from the clustering analysis of the obtained trajectories following the described molecular dynamics simulations. All structures were then optimized by a very efficient DFT M06-2X/6-31+G(d) model employing the implicit SMD solvation with all parameters for pure water. Thermal corrections were extracted from the corresponding frequency calculations so that all presented results correspond to Gibbs free energies at room temperature and normal pressure. All transition state structures were located with the help of the scan procedure, employing both 1D and 2D scans, the latter specifically utilized to exclude the possibility for concerted mechanisms, and then fully optimized as saddle points on the potential energy surface. Apart from the visualization of the obtained negative frequencies, the validity of all transition states was confirmed through IRC calculations in both directions. All the calculations were conducted with the Gaussian 16 software (Frisch et al., 2016).

4. Conclusion

The goal of our study was to obtain information on the rates and mechanisms of ceftriaxone degradation in water, a mixture of water and deuterium oxide, and deuterium oxide itself at the neutral pH (range of 6.7 to 7.6).

Compared to previously published results, all measurements in this study were performed at a therapeutic concentration of 20 mg mL^{-1}. Based on the conducted research, insights have been gained into the behavior of ceftriaxone in an aqueous medium and the effect of the addition of deuterium oxide (D_2O) on its stability.

The results of measurements of assay decrease and increase in the content of impurities have indicated that D_2O significantly reduces the degradation of ceftriaxone in comparison to the degradation in water (H_2O). Mass spectrometry measurements have revealed a plausible pathway for the decomposition of ceftriaxone in water at a pH of around 7. Additionally, a new impurity (ceftriaxone Dimer impurity) has been discovered and described. Quantitative NMR measurements of time-dependent proton spectra revealed the first-order kinetics of ceftriaxone degradation observed also by using the HPLC-based method of initial rates. A clear correlation of degradation rate constant with the solvent composition, i.e., the amount of heavy water, was noticed and the k vs.% D_2O relation could be described by an empirical linear function. The values of solvent kinetic isotope effect determined by both experimental approaches were in a rather good agreement and were found to be temperature dependent. A relatively large SKIE was observed indicating breaking of a water O-H bond involved in the protonation reaction as a rate determining step of ceftriaxone degradation process. That aligns with the results of quantum chemical calculations (DFT) used to calculate the reaction energy profile, as well as to highlight the transition states through which the reaction occurs, providing a plausible ceftriaxone degradation mechanism. It was shown that the β-lactam hydrolysis involves three steps, (i) the rate-limiting nucleophilic water attack onto the β-lactam amide carbon concerted with the proton transfer onto the vicinal carboxylate, which offers a tetrahedral intermediate, (ii) the opening of the β-lactam ring, which generates a negative charge on the liberated amine, and (iii) several acid/base proton transfer equilibria that yield the final product. Its feasibility under neutral conditions is evident in the computed $\Delta G^{\ddagger} = 27.5$ kcal

mol^{-1} and $\Delta G_R = -4.8$ kcal mol^{-1}, and is responsible for a variety of degradation products with a disintegrated β-lactam ring. Further on, the cleavage of the central C–S linker involves the nucleophilic substitution on either the alkyl or the ring carbon atom. In the most feasible scenario, it proceeds by the nucleophilic carboxylate addition to the alkyl carbon atom, which liberates triazine with a concerted formation of lactone, for which the calculated $\Delta G^{\ddagger} = 31.1$ and $\Delta G_R = -9.5$ kcal mol^{-1} indicate a competition with the β–lactam hydrolysis. Based on these models and the way solutions components, solvent molecules and Na^+ ions, are impacting the reaction outcomes, subsequent molecular dynamics simulations elucidated the ceftriaxone behavior in both H_2O and D_2O, and identified reasons for modified stabilities. The latter reside in the fact that, relative to H_2O, D_2O facilitates electrostatic interactions at the catalytic carboxylate and diminishes them at the anionic triazine, which jointly work towards assuring a longer ceftriaxone stability.

Author contributions

The manuscript was written through contributions of all authors. All authors have given approval to the final version of the manuscript.

Funding sources

The results presented here are co-financed by the European Union from the European Regional Development Fund (Liquid antibiotics and active substances with antibiotic-like stabilization mechanisms for intravenous and intramuscular application, KK.01.2.1.02.0175).

Data availability

Data will be made available on request.

Acknowledgment

The authors would like to acknowledge the European Regional Development Fund (Grant No: KK.01.2.1.02.0175) and Xellia pharmaceutical for providing the financial support that made this research possible. Their generosity and commitment to advancing scientific knowledge in our field are greatly appreciated. We would also like to thank our colleagues and collaborators who contributed their time, expertise, and resources to this project

Supplementary materials

Supplementary material associated with this article can be found, in the online version, at doi:10.1016/j.ejps.2023.106461.

References

Abraham, M.J., Murtola, T., Schulz, R., Páll, S., Smith, J.C., Hess, B., Lindah, E., 2015. Gromacs: high performance molecular simulations through multi-level parallelism from laptops to supercomputers. SoftwareX 1–2, 19–25. https://doi.org/10.1016/j.softx.2015.06.001.

Abramović, B.F., Uzelac, M.M., Armaković, S.J., Gašić, U., Četojević-Simin, D.D., Armaković, S., 2021. Experimental and computational study of hydrolysis and photolysis of antibiotic ceftriaxone: degradation kinetics, pathways, and toxicity. Sci. Total Environ. 768, 144991 https://doi.org/10.1016/j.scitotenv.2021.144991.

Aleksić, M., Savić, V., Popović, G., Burić, N., Kapetanović, V., 2005. Acidity constants of cefetamet, cefotaxime and ceftriaxone; the effect of the substituent at C3 position. J. Pharm. Biomed. Anal. 39, 752–756. https://doi.org/10.1016/j.jpba.2005.04.033.

Benoit, R.L., Buisson, C., 1973. Acides forts dans le dimethylsulfoxide. Electrochim. Acta 18, 105–110. https://doi.org/10.1016/0013-4686(73)87018-5.

Bo, G., 2000. Giuseppe Brotzu and the discovery of cephalosporins. Clin. Microbiol. Infect. 6, 6–8. https://doi.org/10.1111/j.1469-0691.2000.tb02032.x.

Bussi, G., Donadio, D., Parrinello, M., 2007. Canonical sampling through velocity rescaling. J. Chem. Phys. 126, 014101 https://doi.org/10.1063/1.2408420.

Chrisment, J., Delpuech, J.J., 1977. Thermodynamic and kinetic acidities in dimethyl sulphoxide. Part 2. Acetylenic compounds. J. Chem. Soc. Perkin Trans. 407 https://doi.org/10.1039/p29770000407, 2.

Darden, T., York, D., Pedersen, L., 1993. Particle mesh Ewald: an N log(N) method for Ewald sums in large systems. J. Chem. Phys. 98, 10089–10092. https://doi.org/10.1063/1.464397.

Deshpande, A.D., Baheti, K.G., Chatterjee, N.R., 2004. Degradation of β-lactam antibiotics. Curr. Sci. 87, 1684–1695.

East, A.L.L., 2018. On the hydrolysis mechanisms of amides and peptides. Int. J. Chem. Kinet. 50, 705–709. https://doi.org/10.1002/kin.21194.

El Seoud, O.A., Bazito, R.C., Sumodjo, P.T., 1997. Kinetic solvent isotope effect: a simple, multipurpose physical chemistry experiment. J. Chem. Educ. 74, 562. https://doi.org/10.1021/ed074p562.

Frau, J., Coll, M., Donoso, J., Muñoz, F., Vilanova, B., García-Blanco, F., 1997. Alkaline and acidic hydrolysis of the β-lactam ring. Electron. J. Theor. Chem. 2, 56–65. https://doi.org/10.1002/ejtc.34.

Frisch, M.J., Trucks, G.W., Schlegel, H.B., Scuseria, G.E., Robb, M.A., Cheeseman, J.R.., Scalmani, G.., Barone, V.., Petersson, G.A., Nakatsuji, H., Li, X., Caricato, M., 2016. Gaussian C.01. Gaussian, Inc., Wallingford CT.

Hamilton-Miller, J., 2000. Sir Edward Abraham's contribution to the development of the cephalosporins: a reassessment. Int. J. Antimicrob. Agents 15, 179–184. https://doi.org/10.1016/S0924-8579(00)00179-5.

Jiang, M., Wang, L., Ji, R., 2010. Biotic and abiotic degradation of four cephalosporin antibiotics in a lake surface water and sediment. Chemosphere 80, 1399–1405. https://doi.org/10.1016/j.chemosphere.2010.05.048.

Linse, J.-.B., Hub, J.S., 2021. Three- and four-site models for heavy water: SPC/E-HW, TIP3P-HW, and TIP4P/2005-HW. J. Chem. Phys. 154, 194501 https://doi.org/10.1063/5.0050841.

Mackle, H., McClean, R.T.B., 1962. Studies in the thermochemistry of organic sulphides. Part 4.—Heat of formation of the mercaptyl radical. Trans. Faraday Soc. 58, 895–899. https://doi.org/10.1039/TF9625800895.

Mitchell, S.M., Ullman, J.L., Teel, A.L., Watts, R.J., 2014. PH and temperature effects on the hydrolysis of three β-lactam antibiotics: ampicillin, cefalotin and cefoxitin. Sci. Total Environ. 466–467, 547–555. https://doi.org/10.1016/j.scitotenv.2013.06.027.

Parrinello, M., Rahman, A., 1981. Polymorphic transitions in single crystals: a new molecular dynamics method. J. Appl. Phys. 52, 7182–7190. https://doi.org/10.1063/1.328693.

Richards, D.M., Heel, R.C., Brogden, R.N., Speight, T.M., Avery, G.S., 1984. Ceftriaxone a review of its antibacterial activity, pharmacological properties and therapeutic use. Drugs 27, 469–527. https://doi.org/10.2165/00003495-198427060-00001.

Slebocka-Tilk, H., Sauriol, F., Monette, M., Brown, R.S., 2002. Aspects of the hydrolysis of formamide: revisitation of the water reaction and determination of the solvent deuterium kinetic isotope effect in base. Can. J. Chem. 80, 1343–1350. https://doi.org/10.1139/v02-166.

Tian, Y., Lu, L., Chang, Y., Zhang, D., Li, J., Feng, Y.C., Hu, C.Q., 2015. Identification of a new isomer from a reversible isomerization of ceftriaxone in aqueous solution. J. Pharm. Biomed. Anal. 102, 326–330. https://doi.org/10.1016/j.jpba.2014.07.040.

Wan, P., Modro, T.A., Yates, K., 1980. The kinetics and mechanism of acid catalysed hydrolysis of lactams. Can. J. Chem. 58, 2423–2432. https://doi.org/10.1139/v80-391.

Waterman, K.C., Adami, R.C., Alsante, K.M., Antipas, A.S., Arenson, D.R., Carrier, R., Hong, J., Landis, M.S., Lombardo, F., Shah, J.C., Shalaev, E., Smith, S.W., Wang, H., 2002. Hydrolysis in pharmaceutical formulations. Pharm. Dev. Technol. 7, 113–146. https://doi.org/10.1081/PDT-120003494.

Wei, W.M., Xu, Y.L., Zheng, R.H., Zhao, T., Fang, W., De Qin, Y., 2021. Theoretical study on the mechanism of the acylate reaction of β-lactamase. ACS Omega 6, 12598–12604. https://doi.org/10.1021/acsomega.1c00592.

Yamana, T., Tsuji, A., 1976. Comparative stability of cephalosporins in aqueous solution: kinetics and mechanisms of degradation. J. Pharm. Sci. 65, 1563–1574. https://doi.org/10.1002/jps.2600651104.

Yamana, T., Tsuji, A., Kiya, E., Miyamoto, E., 1977. Physicochemical properties of β-lactam Antibacterials: deuterium solvent isotope effect on penicillin G degradation rate. J. Pharm. Sci. 66, 861–866. https://doi.org/10.1002/jps.2600660632.

Zając, M., Muszalska, I., 1998. Mechanism of ceftriaxone degradation in aqueous solution. Acta Pol. Pharm. - Drug Res.

Zhang, S., 2012. A reliable and efficient first principles-based method for predicting pKa values. 4. organic bases. J. Comput. Chem. 33, 2469–2482. https://doi.org/10.1002/jcc.23068.